Malaria Parasite Structural Biology

- **Unique pathogen protein for drug development?**
- **'Equity' justifies the targets: examples**
- **Conserved targets are valuable: STOPP**

Amit Sharma
New Delhi, India

Aminoacylation:
a two-step reaction

Genetic code translation

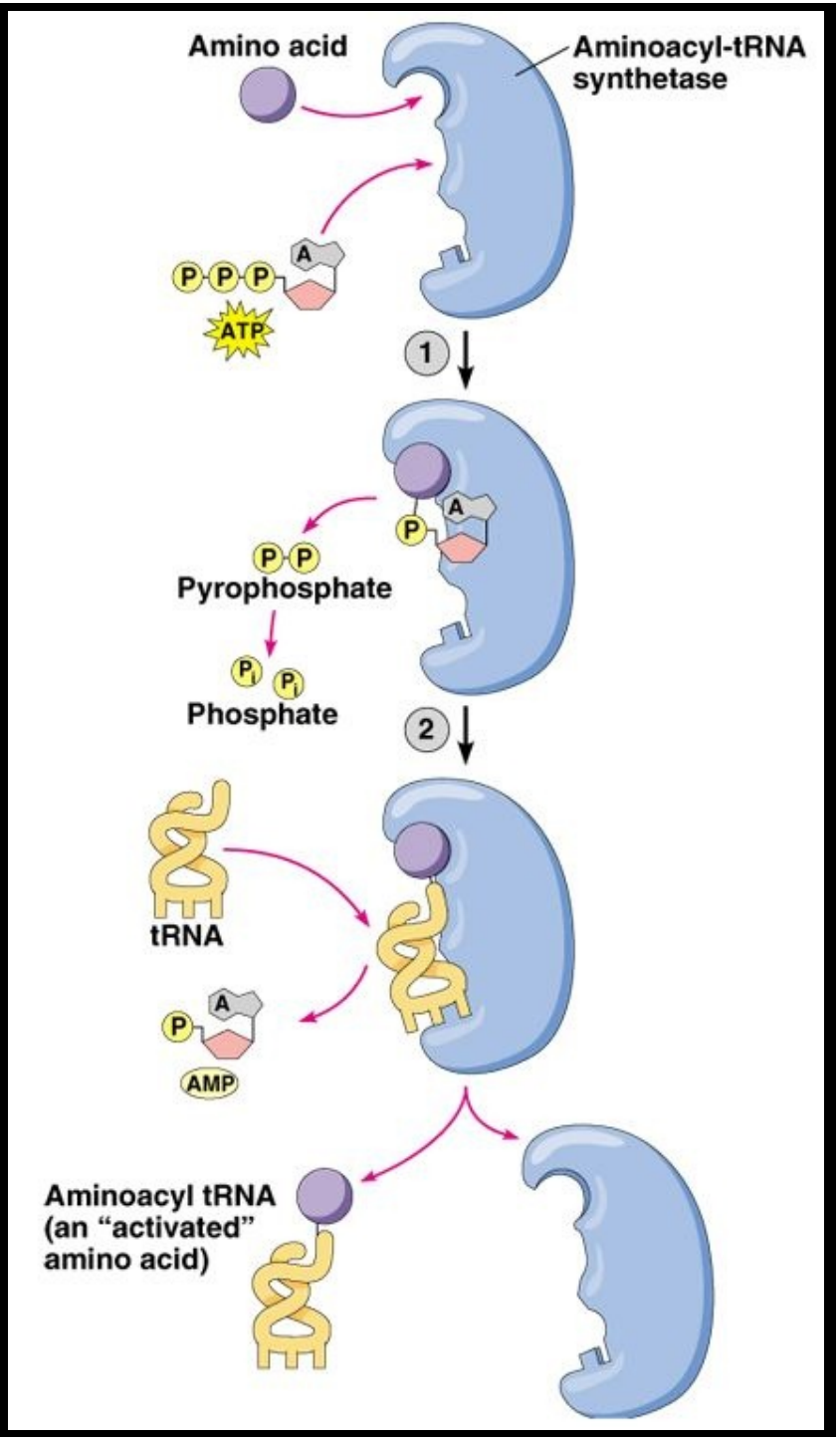

Staph infections and bactroban

Mupirocin is an antibiotic

Selective binding to bacterial IRS

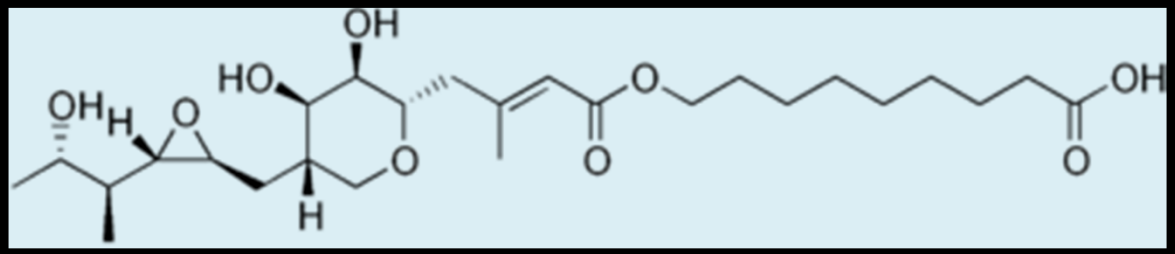

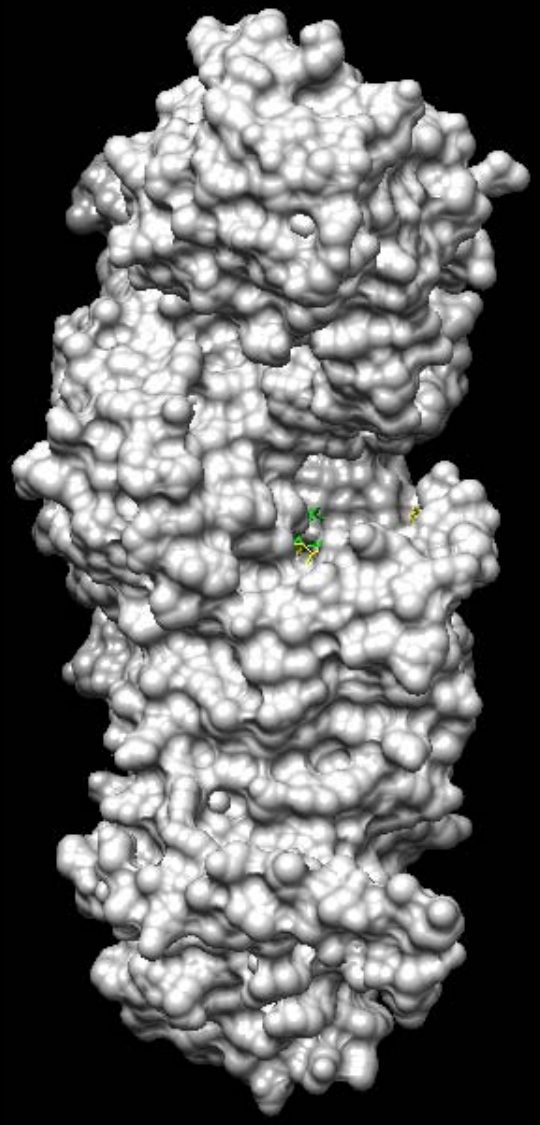

Silvian et al., 1999; Nakama et al., 2001

Onychomycosis: fungal nail infection

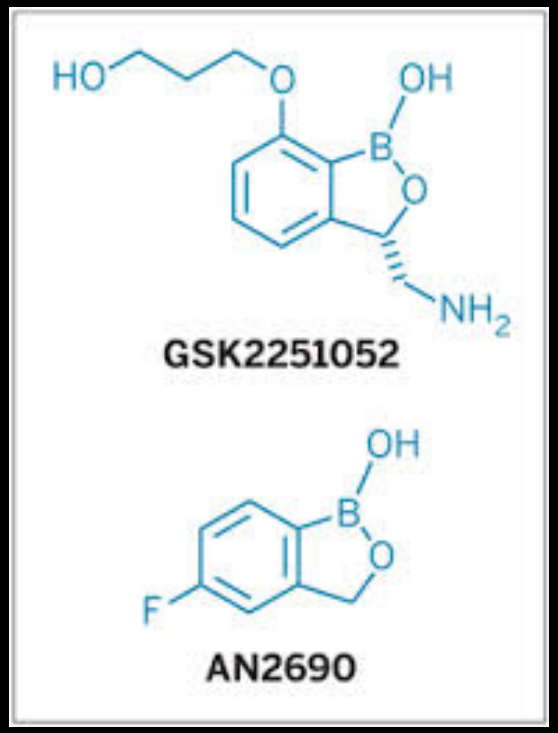

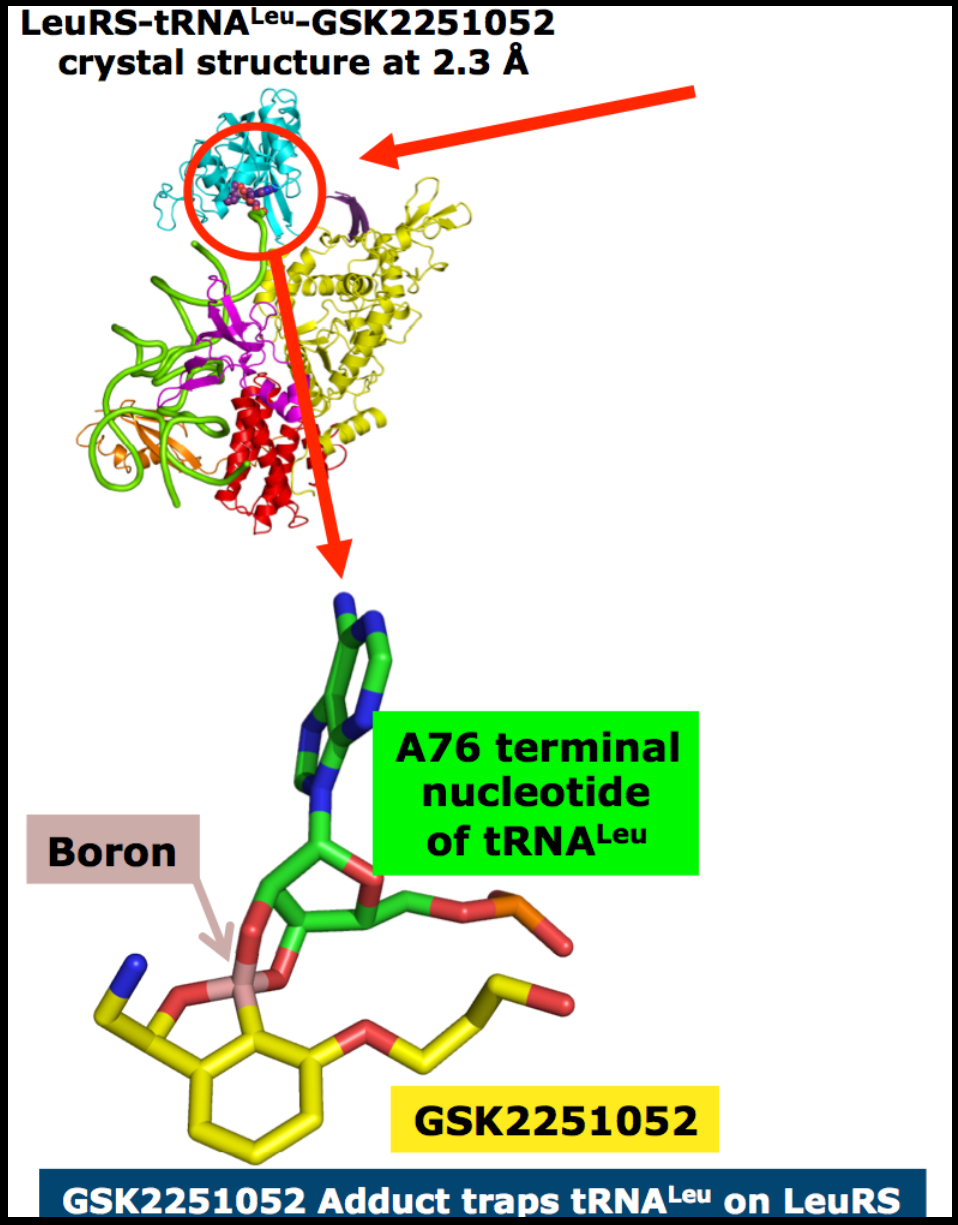

Baker *et al.(2006) , Rock et al., 2007*

Plasmodium falciparum aaRSs

Compartments: 3
aaRSs: 36

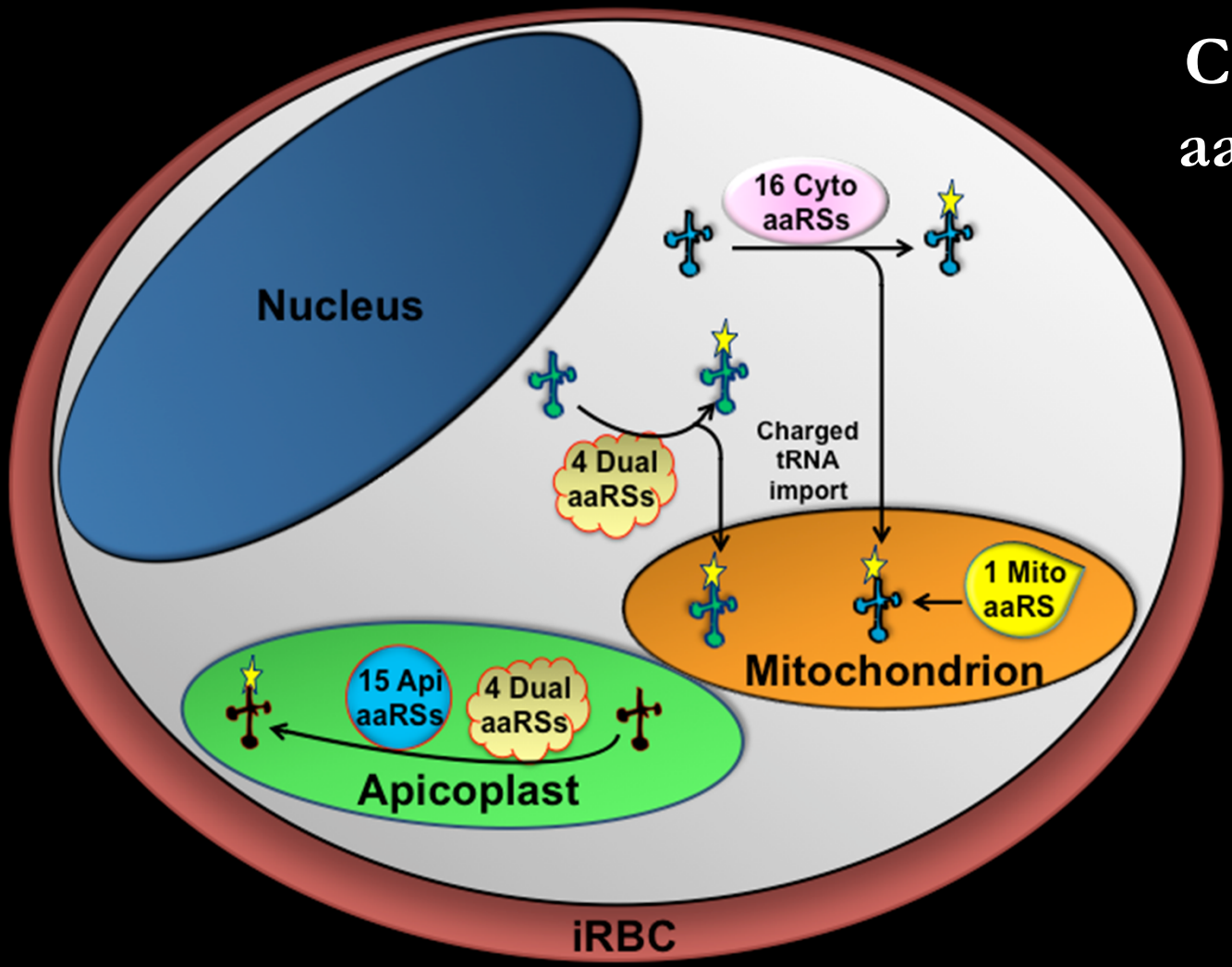

- *Dual localization of single copy aaRS*
- tRNA trafficking

Sharma et al 2015

STOPP via cladosporin: example 1

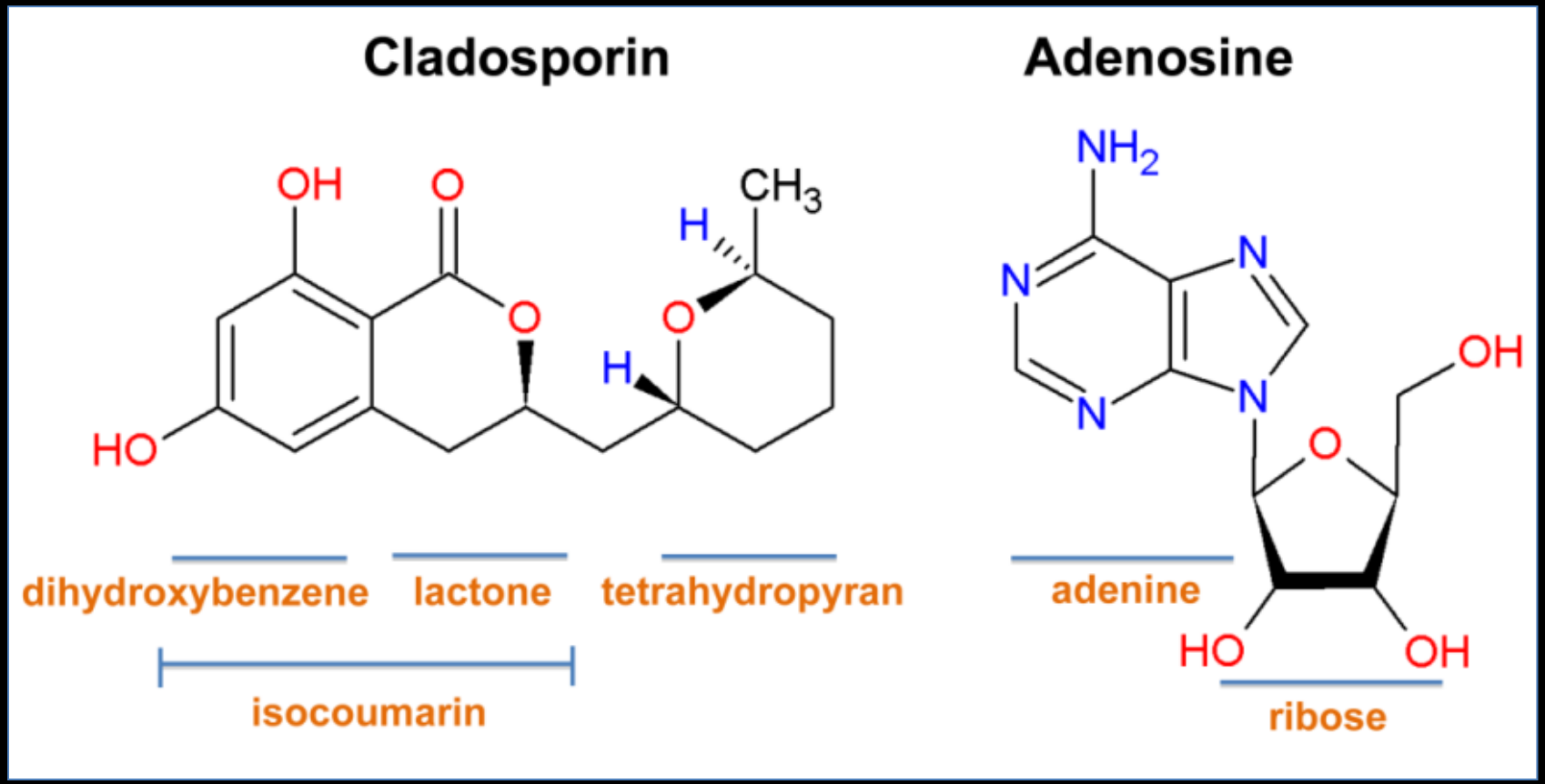

Dominic et al, 2012; Khan et al 2013, Khan et al 2014

Selectivity of cladosporin

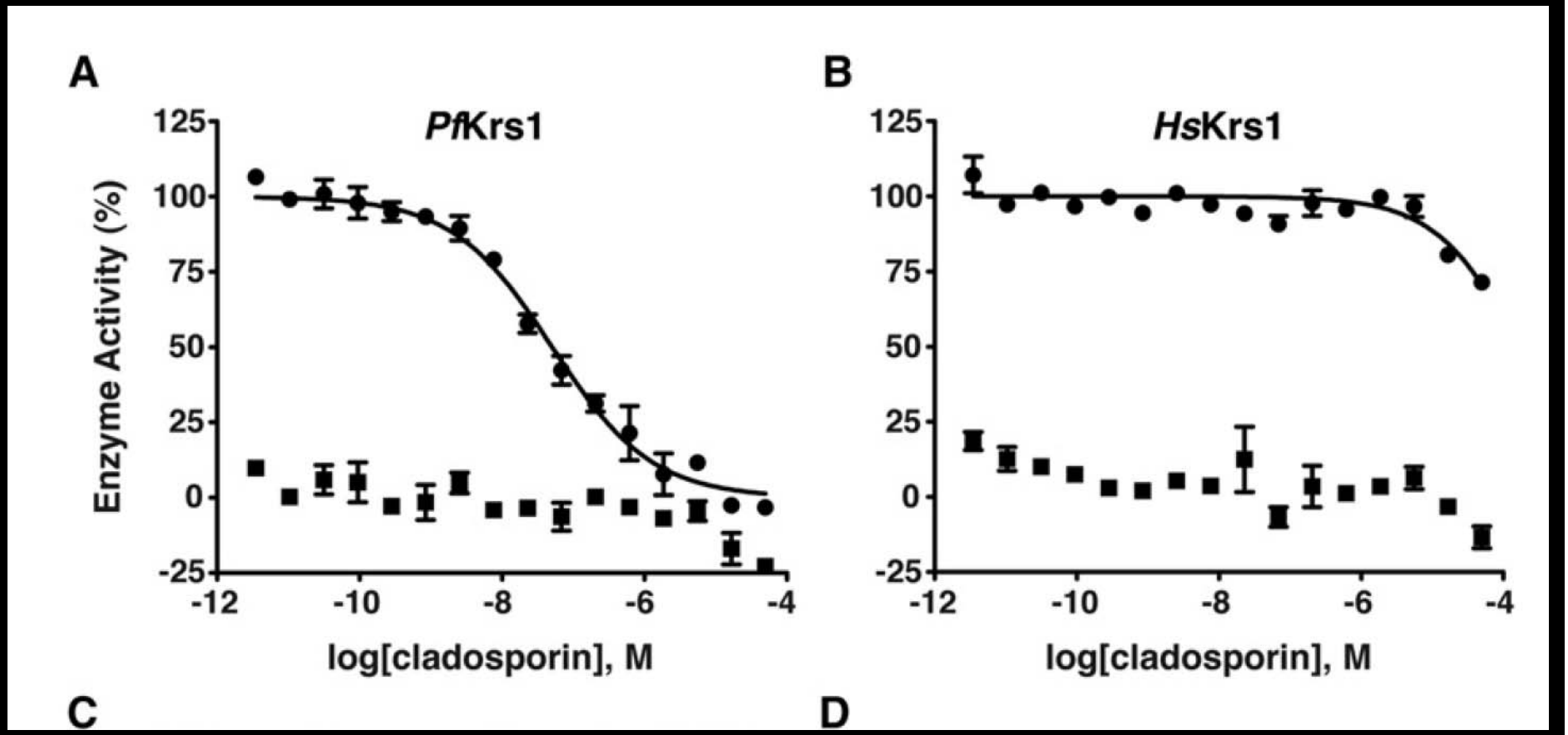

Dominic et al, 2012

Selectivity of cladosporin

Table 2. Summary of Amino Acid Conservation at Key Residues in the ATP Pocket of Krs1 and Corresponding IC_{50} Value of Cladosporin

	Cladosporin Inhibition		Key Active Site Residues[a]	
Organism	IC_{50} (μM)	MIC[b] (μg/ml)	Position 324	Position 340
Plasmodium falciparum[c]	0.04–0.08		Val	Ser
Plasmodium yoelii[d]	0.04		Val	Ser
Trypanosoma brucei	2.05		Val	Thr
Leishmania donovani	2.56		Val	Thr
Toxoplasma gondii	2.63		Asn	Ala
Homo sapiens	>10		Gln	Thr
Saccharomyces cerevisiae	30–110		Gln	Thr
Escherichia coli		>100	Asn	Met
Bacillus stearothermophilus		>100	Val	Met

Dominic et al, 2012

PfKRS binding to cladosporin

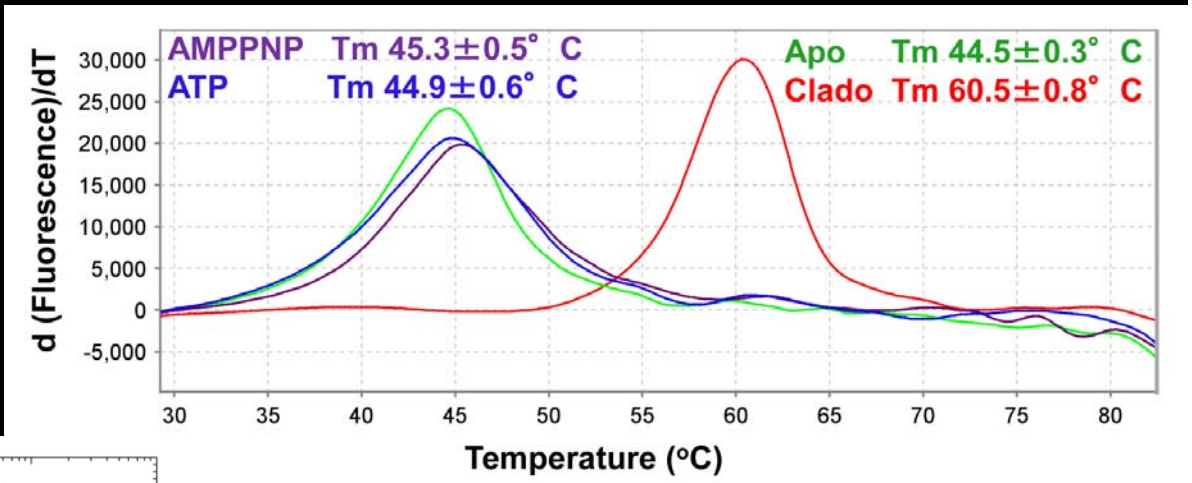

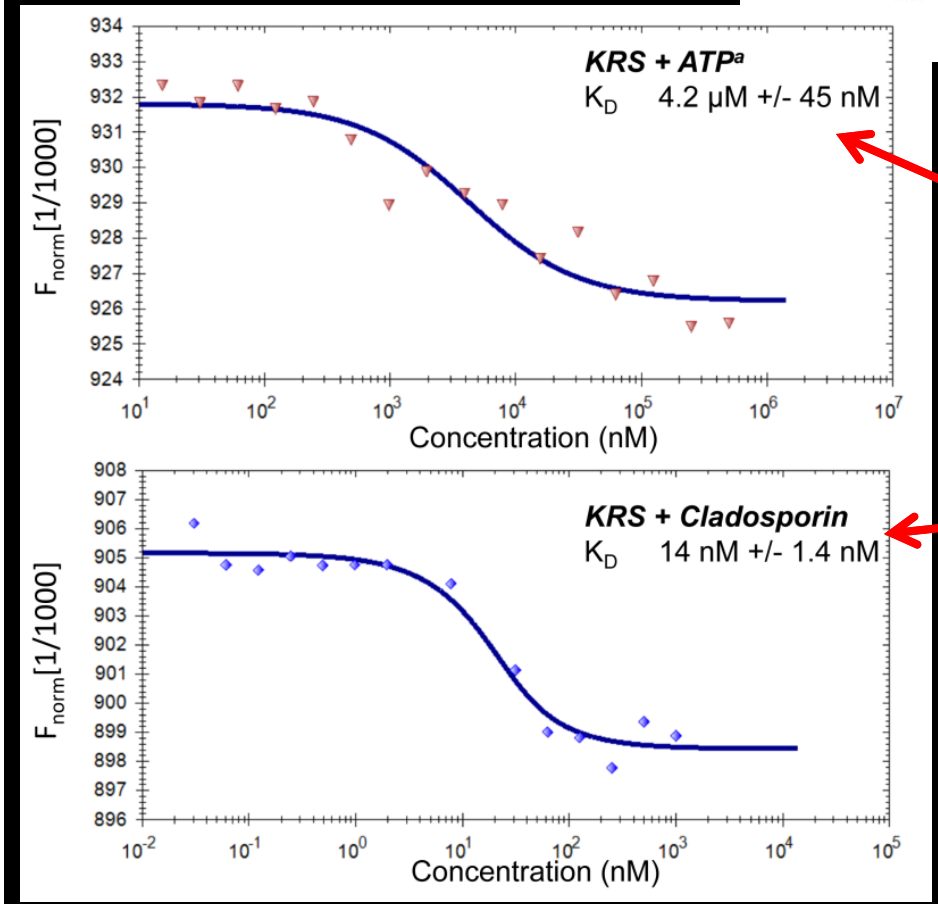

~300x

Khan et al., 2013; Khan et al., 2014

KRS + Cladosporin

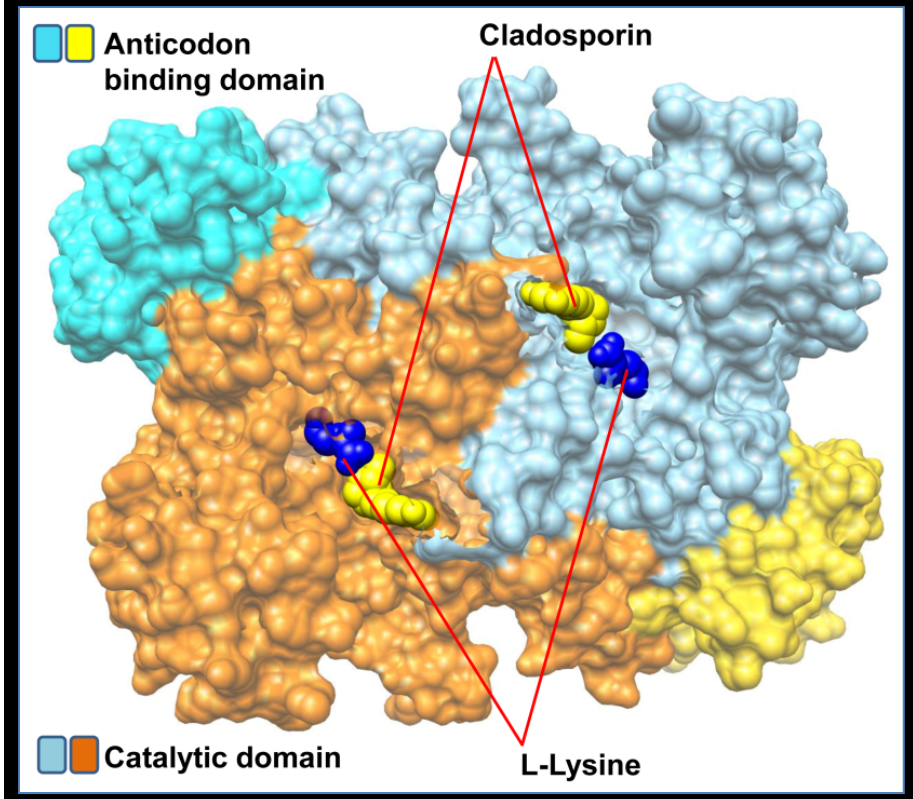

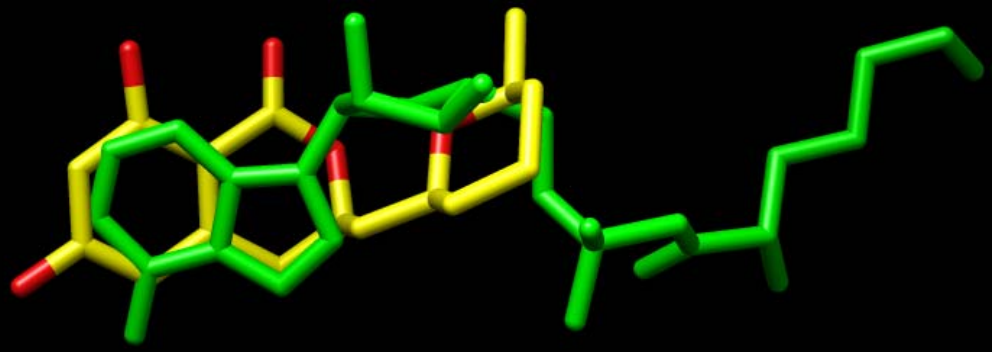

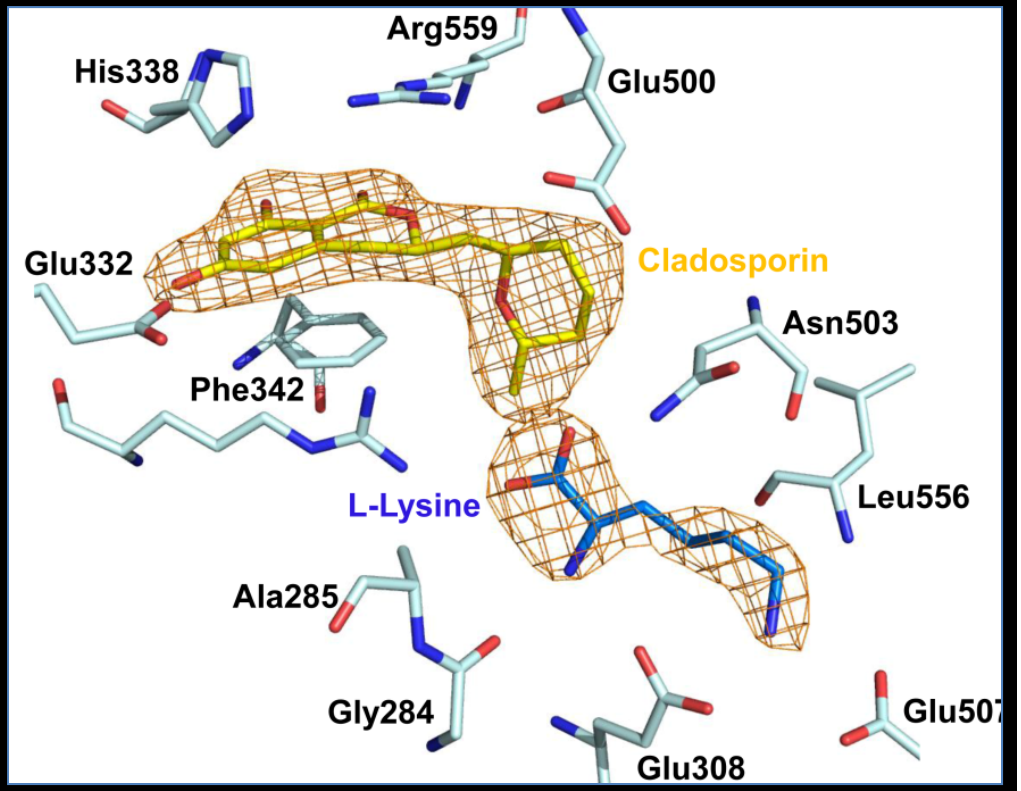

Khan et al., 2013; Khan et al., 2014

Basis of cladosporin selectivity

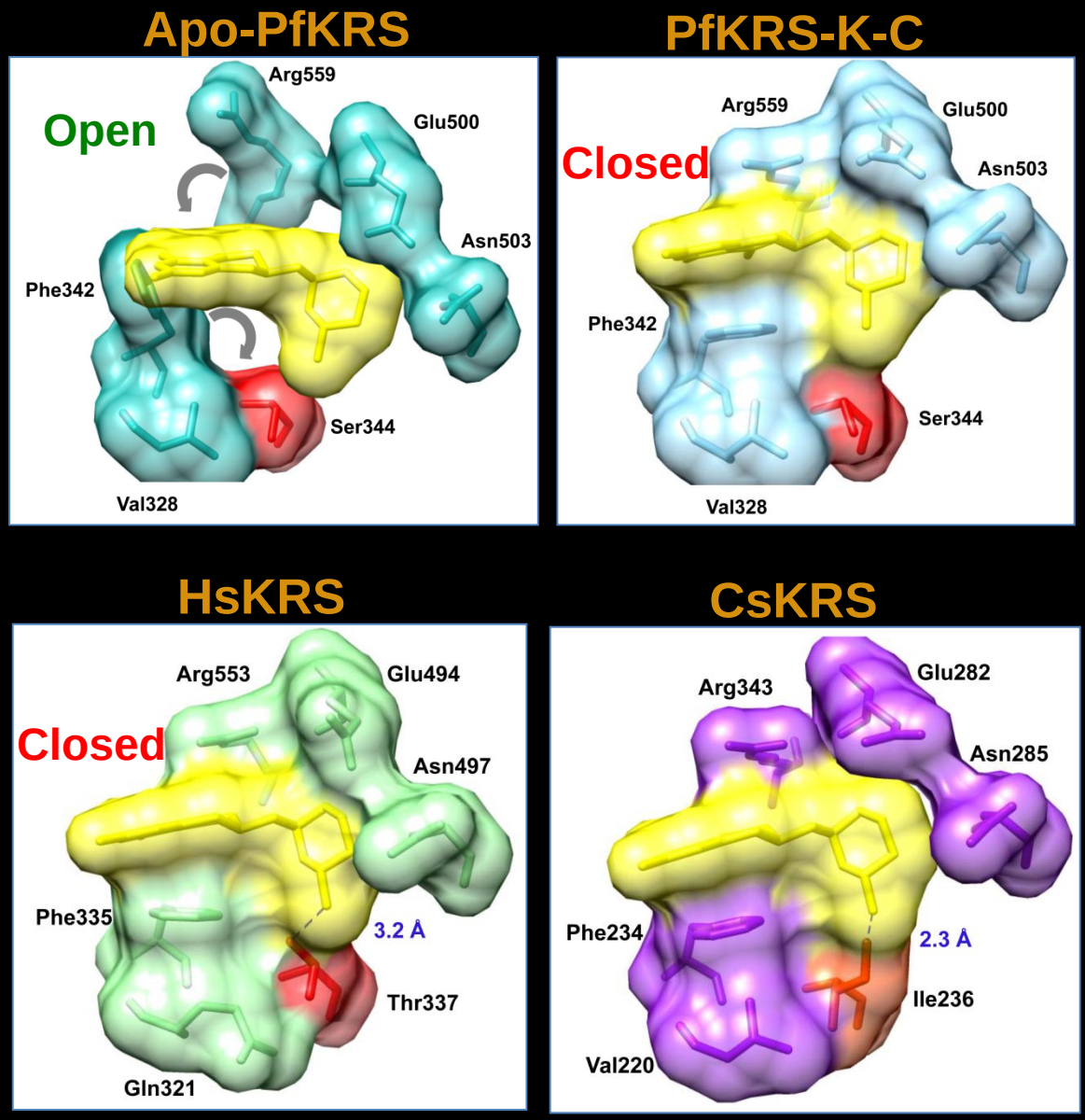

Khan et al., 2013; Khan et al., 2014

Resistant versus sensitive KRSs

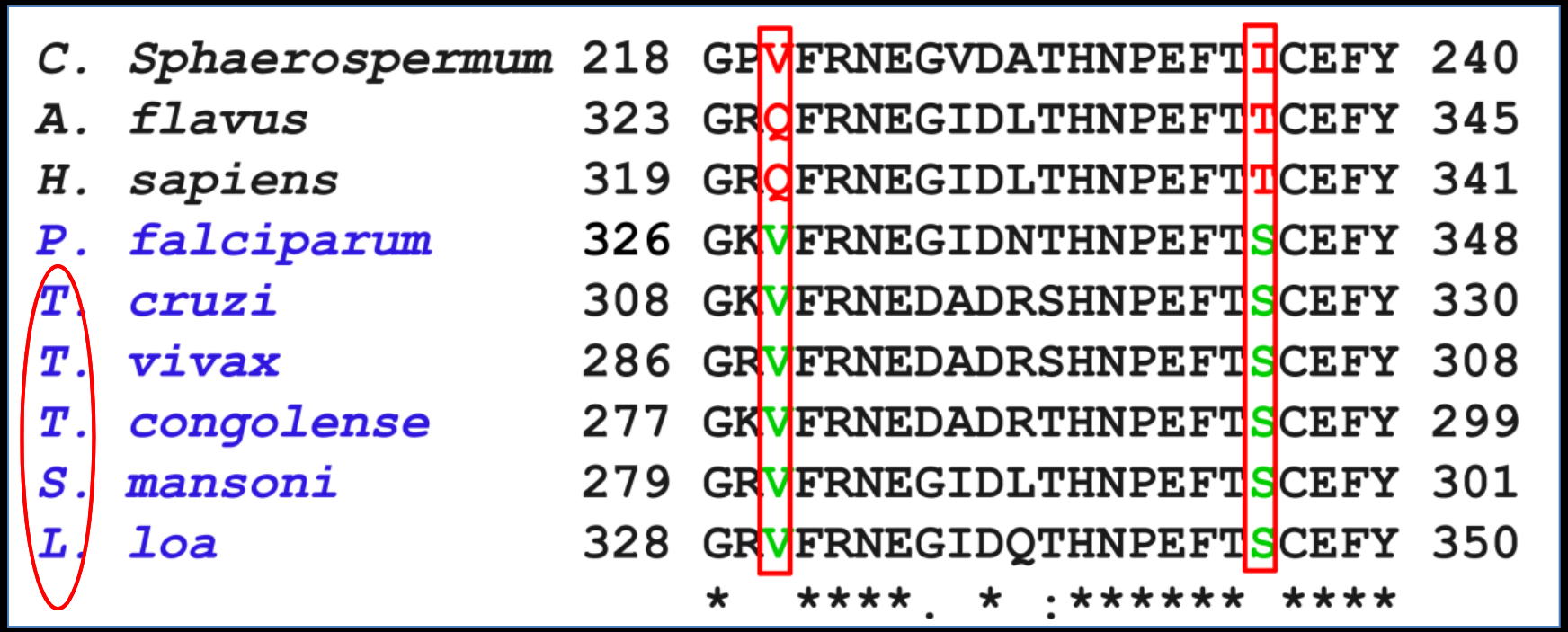

Pathogens

Khan et al., 2013; Khan et al., 2014

STOPP: Structure-based Targeting of Orthologous Pathogen Proteins

Jain et al, 2016, 2017

STOPP via cladosporin: example 1

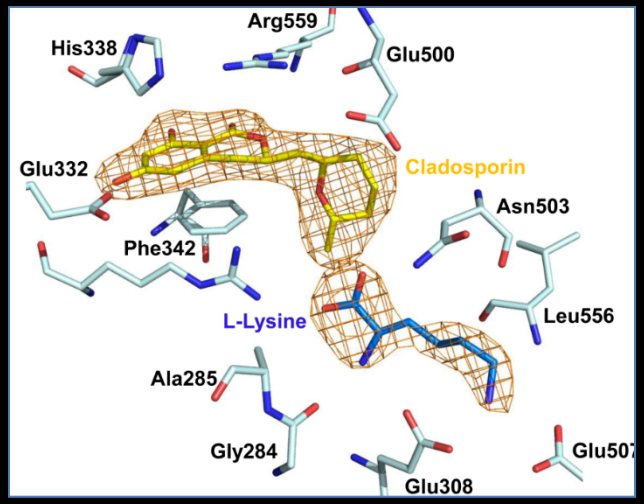


```
C. Sphaerospermum 218 GPVFRNEGVDATHNPEFTICEFY 240
A. flavus         323 GRQFRNEGIDLTHNPEFTTCEFY 345
H. sapiens        319 GRQFRNEGIDLTHNPEFTTCEFY 341
P. falciparum     326 GKVFRNEGIDNTHNPEFTSCEFY 348
T. cruzi          308 GKVFRNEDADRSHNPEFTSCEFY 330
T. vivax          286 GRVFRNEDADRSHNPEFTSCEFY 308
T. congolense     277 GKVFRNEDADRTHNPEFTSCEFY 299
S. mansoni        279 GRVFRNEGIDLTHNPEFTSCEFY 301
L. loa            328 GRVFRNEGIDQTHNPEFTSCEFY 350
                      *  ****. * :****** ****
```

Structure with drug

Conserved pathogen active sites

Arvind et al, 2016

Worm KRSs inhibited by cladosporin

***Ll*KRS**

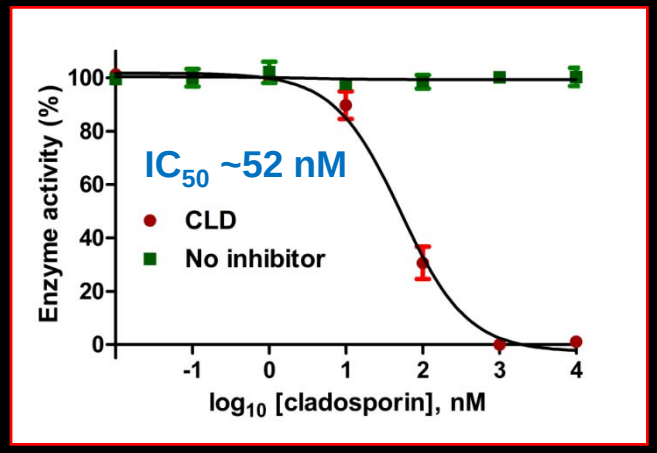

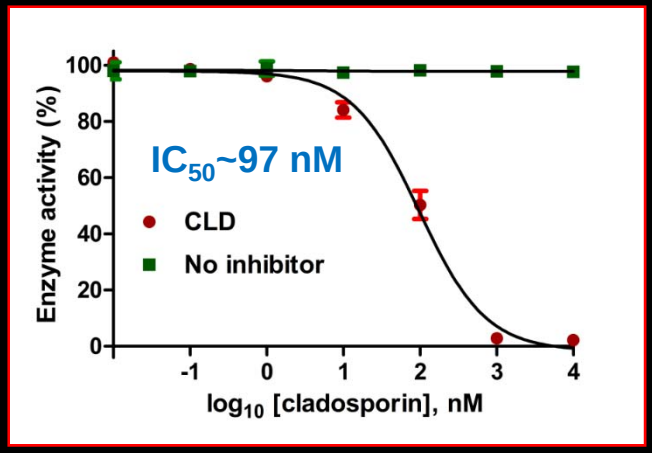

***Sm*KRS**

STOPP via febrifugine: example 2

Febrifugine (FF): Chinese herb: treating malaria-induced fever

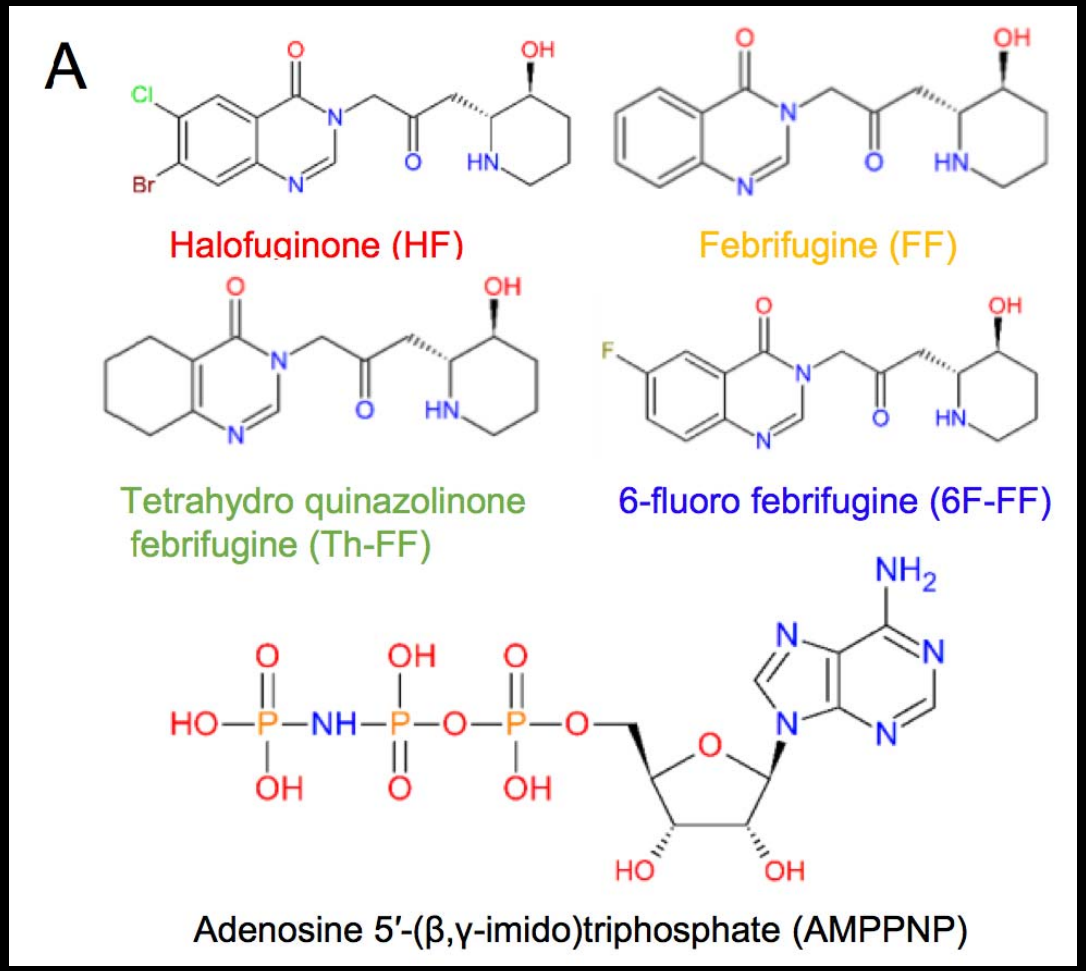

4-quinazolinone

Piperidine

Keller et al, 2011

Febrifugine derivatives and parasite inhibition

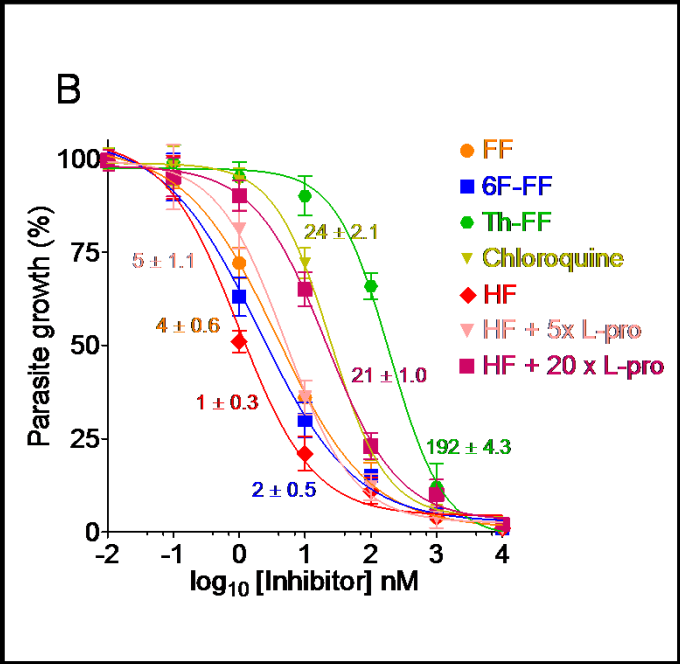

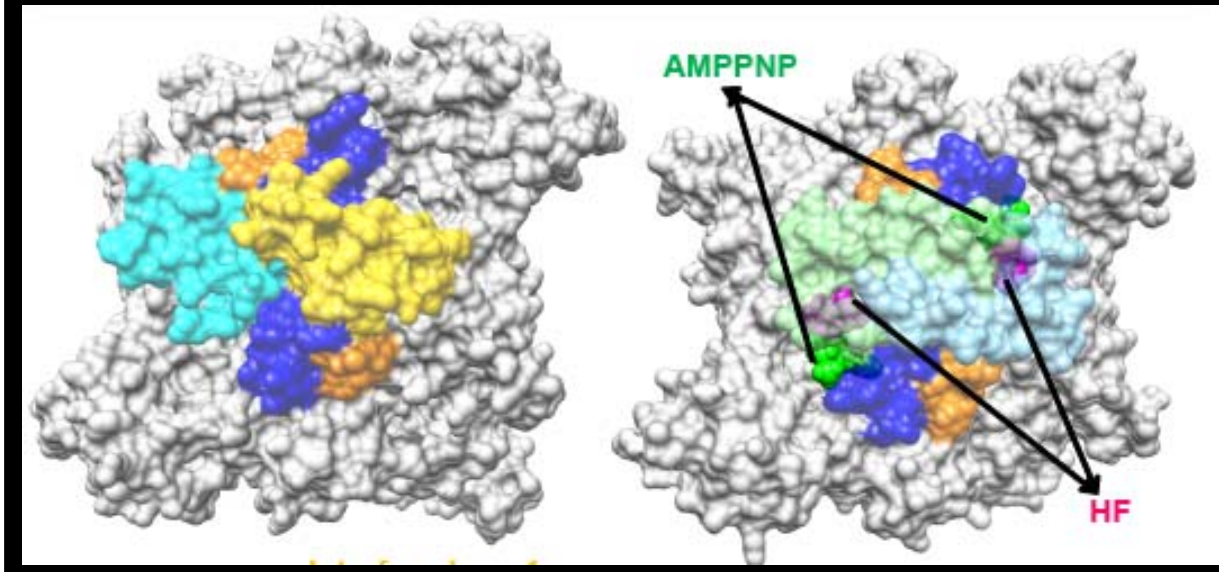

Table 1. Summary of the Inhibition and T_m Values of Tested Inhibitors in *Plasmodium falciparum*

S. No.	Inhibitor	Enzyme Inhibition IC_{50} (nM)	Parasite (3D7) Inhibition EC_{50} (nM)	Change in Melting Temperature ΔT_m (°C)		Mammalian Cells EC_{50} (nM)	Selectivity Index
				Only Drug	Drug with AMPPNP		
1	HF	9 ± 0.6	1 ± 0.3	15 ± 0.6	40 ± 0.7	150 ± 9[a]	150
2	FF	24 ± 1.7	4 ± 0.6	1.5 ± 0.2	33 ± 0.5	450 ± 20[b]	118
3	6F-FF	13 ± 1.5	2 ± 0.5	0.5 ± 0.1	35 ± 0.5	205 ± 12[b]	108
4	Th-FF	352 ± 7.2	192 ± 4.3	1 ± 0.1	31 ± 0.4	190000 ± 1100[c]	934

Jain et al., 2014, Jain et al. 2015

STOPP via febrifugine

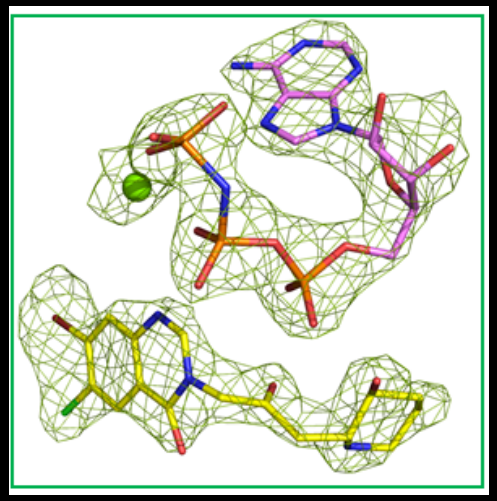

Structure with drug

+

	325	331	335	338	339	358	359	361	365	390	407	409	411	454	460	478	480	482	486	508	509	510
Pf	L	H	F	E	V	P	T	E	Y	R	W	E	H	F	T	T	H	L	F	S	W	G
PV	L	H	F	E	V	P	T	E	Y	R	W	E	H	F	T	T	H	L	F	S	W	G
Cp	L	H	F	E	V	P	T	E	Y	R	W	E	H	F	T	T	H	L	F	S	W	G
Et	L	H	F	E	V	P	T	E	Y	R	W	E	H	F	T	T	H	L	F	S	W	G
Lm	L	H	F	E	V	P	T	E	Y	R	W	E	H	F	T	T	H	L	F	S	W	G
Tb	L	H	F	E	V	P	T	E	Y	R	W	E	H	F	T	T	H	L	F	S	W	G
Tg	L	H	F	E	V	P	T	E	Y	R	W	E	H	F	T	T	H	L	F	S	W	G
Af	L	H	F	E	V	P	T	E	Y	R	W	E	H	F	T	T	H	L	F	S	W	G
Ca	L	H	F	E	V	P	T	E	Y	R	W	E	H	F	T	T	H	L	F	S	W	G
Hs	L	H	F	E	V	P	T	E	Y	R	W	E	H	F	T	T	H	L	F	S	W	G

+

Conserved pathogen active sites

STOPP via febrifugine

Leishmaniasis, toxoplasmosis, cryptosporidiosis…

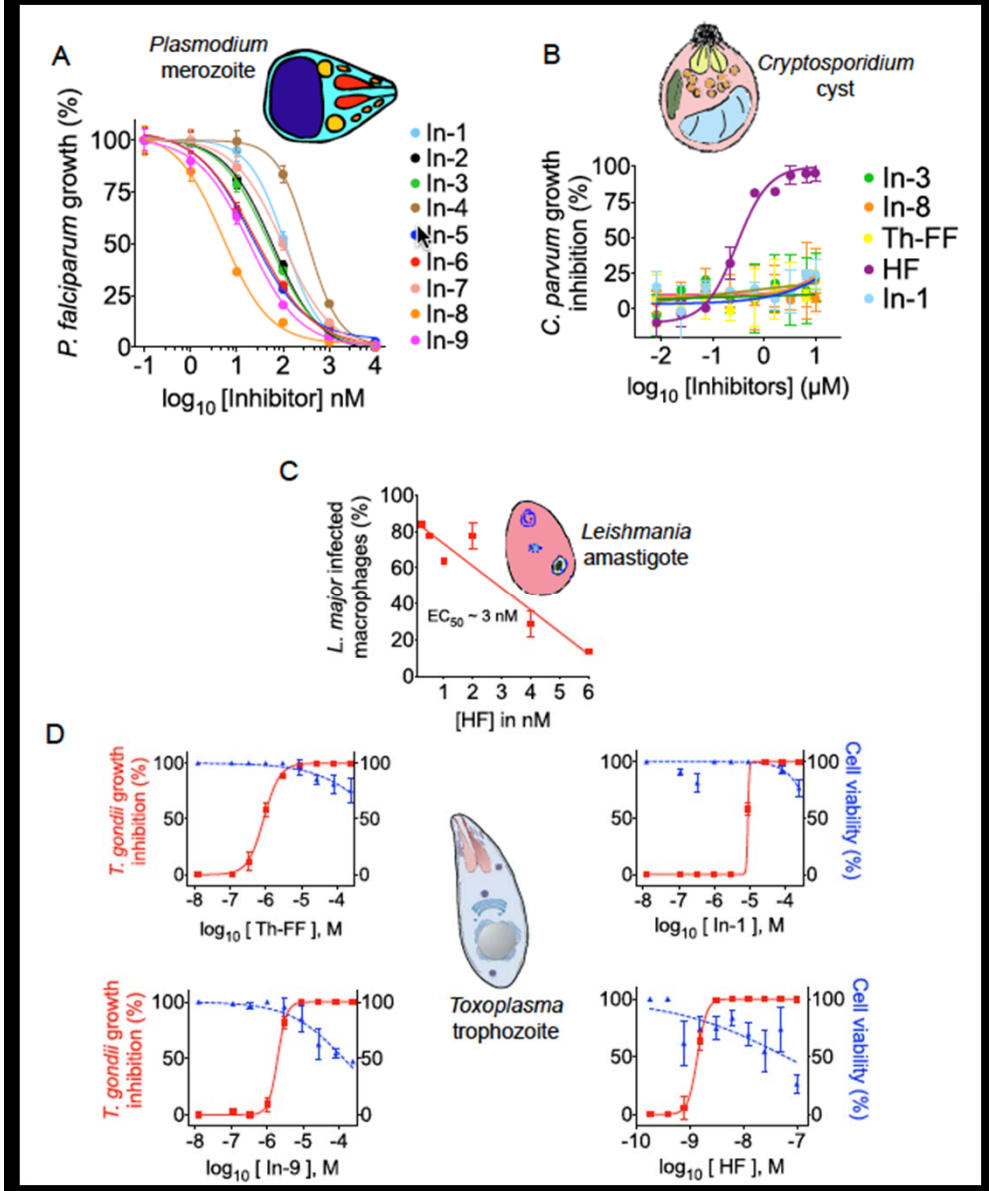

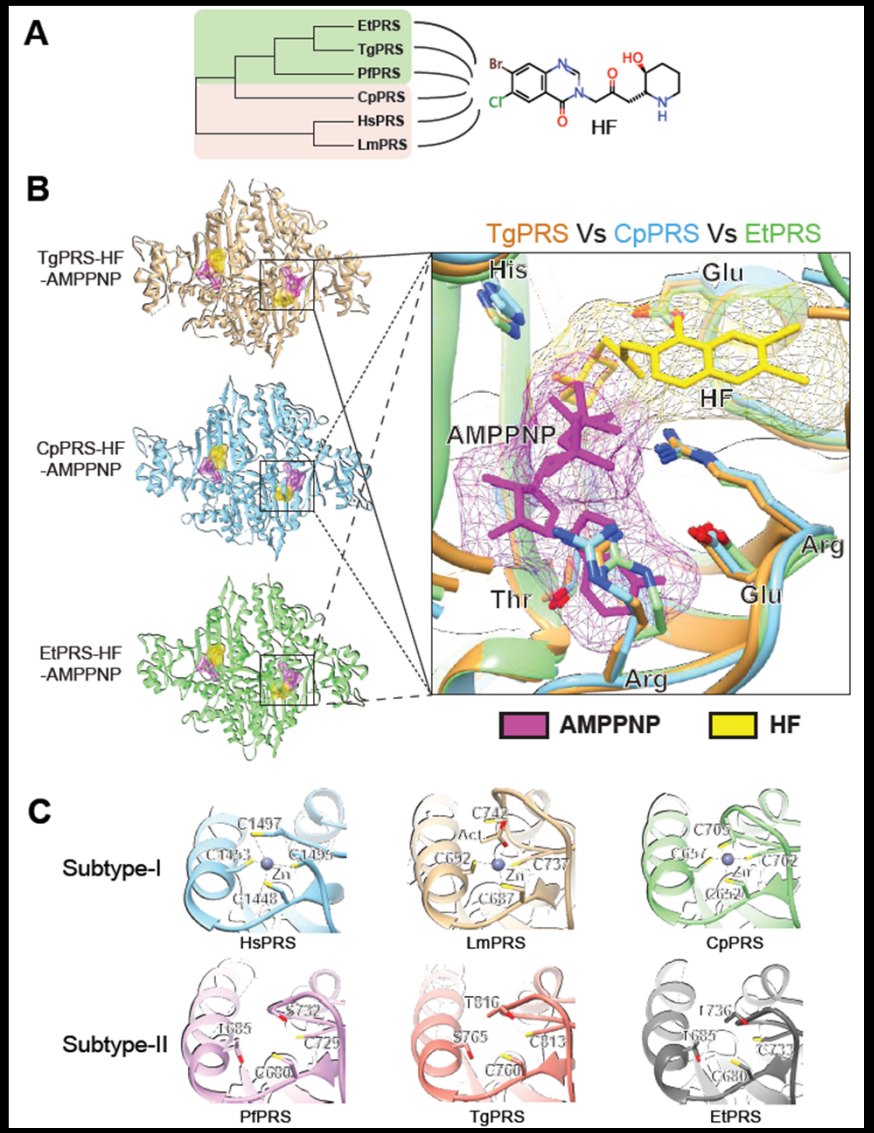

Jain et al. 2017

STOPP via DOS compounds: example 3

ARTICLE

doi:10.1038/nature19804

Diversity-oriented synthesis yields novel multistage antimalarial inhibitors

Nobutaka Kato[1]*, Eamon Comer[1]*, Tomoyo Sakata-Kato[2], Arvind Sharma[3], Manmohan Sharma[3], Micah Maetani[1,4], Jessica Bastien[1], Nicolas M. Brancucci[2], Joshua A. Bittker[1], Victoria Corey[5], David Clarke[2], Emily R. Derbyshire[1,6,7], Gillian L. Dornan[8], Sandra Duffy[9], Sean Eckley[10], Maurice A. Itoe[2], Karin M. J. Koolen[11], Timothy A. Lewis[1], Ping S. Lui[2], Amanda K. Lukens[1,2], Emily Lund[2], Sandra March[1,12], Elamaran Meibalan[2], Bennett C. Meier[1,4], Jacob A. McPhail[8], Branko Mitasev[10], Eli L. Moss[1], Morgane Sayes[1], Yvonne Van Gessel[10], Mathias J. Wawer[1], Takashi Yoshinaga[13], Anne-Marie Zeeman[14], Vicky M. Avery[9], Sangeeta N. Bhatia[1,12], John E. Burke[8], Flaminia Catteruccia[2], Jon C. Clardy[1,6], Paul A. Clemons[1], Koen J. Dechering[11], Jeremy R. Duvall[1], Michael A. Foley[1], Fabian Gusovsky[10], Clemens H. M. Kocken[14], Matthias Marti[2], Marshall L. Morningstar[1], Benito Munoz[1], Daniel E. Neafsey[1], Amit Sharma[3], Elizabeth A. Winzeler[5], Dyann F. Wirth[1,2], Christina A. Scherer[1] & Stuart L. Schreiber[1,4]

Antimalarial drugs have thus far been chiefly derived from two sources—natural products and synthetic drug-like compounds. Here we investigate whether antimalarial agents with novel mechanisms of action could be discovered using a diverse collection of synthetic compounds that have three-dimensional features reminiscent of natural products and are underrepresented in typical screening collections. We report the identification of such compounds with both previously reported and undescribed mechanisms of action, including a series of bicyclic azetidines that inhibit a new antimalarial target, phenylalanyl-tRNA synthetase. These molecules are curative in mice at a single, low dose and show activity against all parasite life stages in multiple *in vivo* efficacy models. Our findings identify bicyclic azetidines with the potential to both cure and prevent transmission of the disease as well as protect at-risk populations with a single oral dose, highlighting the strength of diversity-oriented synthesis in revealing promising therapeutic targets.

Kato et al 2016

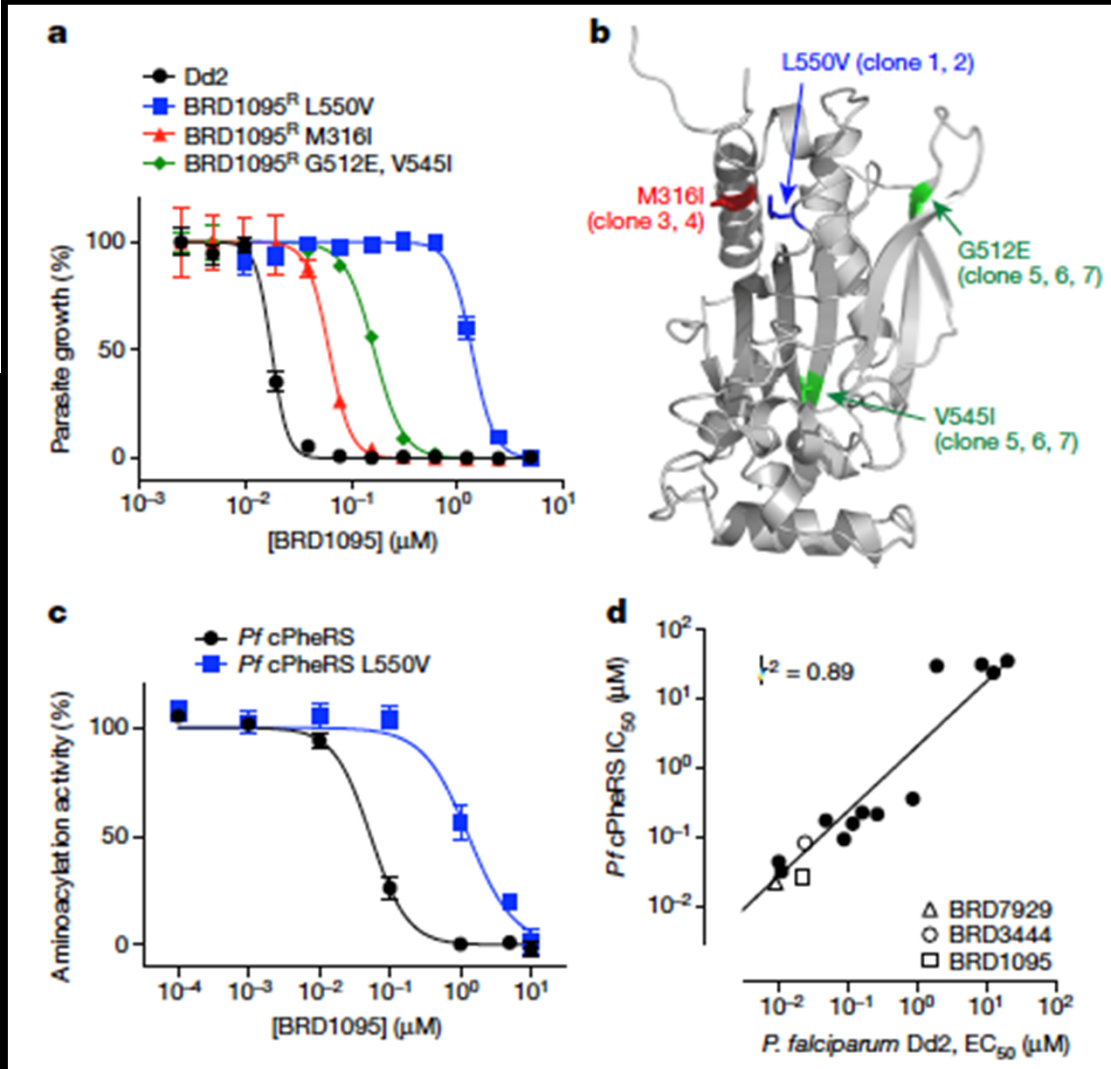

Figure 3 | The bicyclic azetidine series targets the cytoplasmic *Pf*

STOPP via GNF compounds: example 4

LETTER

doi:10.1038/nature19339

Proteasome inhibition for treatment of leishmaniasis, Chagas disease and sleeping sickness

Shilpi Khare[1]*, Advait S. Nagle[1]*, Agnes Biggart[1], Yin H. Lai[1], Fang Liang[1], Lauren C. Davis[1], S. Whitney Barnes[1], Casey J. N. Mathison[1], Elmarie Myburgh[2,3], Mu-Yun Gao[1], J. Robert Gillespie[4], Xianzhong Liu[1], Jocelyn L. Tan[1], Monique Stinson[1], Ianne C. Rivera[1], Jaime Ballard[1], Vince Yeh[1], Todd Groessl[1], Glenn Federe[1], Hazel X. Y. Koh[5], John D. Venable[1], Badry Bursulaya[1], Michael Shapiro[1], Pranab K. Mishra[1], Glen Spraggon[1], Ansgar Brock[1], Jeremy C. Mottram[2,3], Frederick S. Buckner[4], Srinivasa P. S. Rao[5], Ben G. Wen[1], John R. Walker[1], Tove Tuntland[1], Valentina Molteni[1], Richard J. Glynne[1] & Frantisek Supek[1]

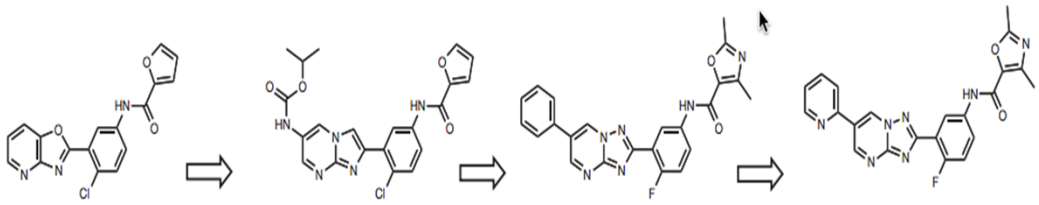

GNF5343 (hit from screen)		GNF2636		GNF3849		GNF6702	
L. donovani EC_{50}	= 7.3 ± 0.6 μM	*L. donovani* EC_{50}	= 350 ± 7.1 nM	*L. donovani* EC_{50}	= 71 ± 3.0 nM	*L. donovani* EC_{50}	= 18 ± 1.8 nM
T. brucei EC_{50}	= 150 ± 7.5 nM	*T. brucei* EC_{50}	= 79 ± 2.9 nM	*T. brucei* EC_{50}	= 22 ± 2.0 nM	*T. brucei* EC_{50}	= 70 ± 1.5 nM
T. cruzi EC_{50}	= 75 ± 0.8 nM	*T. cruzi* EC_{50}	= 55 ± 12 nM	*T. cruzi* EC_{50}	= 16 ± 0.9 nM	*T. cruzi* EC_{50}	= 120 ± 2.6 nM
3T3 CC_{50}	= 17 ± 0.9 μM	3T3 CC_{50}	= 9.0 ± 0.9 μM	3T3 CC_{50}	= 5.0 ± 1.3 μM	3T3 CC_{50}	> 20 μM
Macrophage CC_{50}	> 50 μM	Macrophage CC_{50}	= 14 ± 2.1 μM	Macrophage CC_{50}	= 9.3 ± 1.7 μM	Macrophage CC_{50}	> 50 μM
F	< 5%	F	= ND	F	= 34%	F	= 34%
CL	= ND	CL	= ND	CL	= 2.5 ml min^{-1} kg^{-1}	CL	= 2.0 ml min^{-1} kg^{-1}

Figure 1 | Chemical evolution of GNF6702 from the phenotypic hit GNF5343. *Leishmania donovani*, amastigotes proliferating within primary mouse macrophages; *T. brucei*, the bloodstream form trypomastigotes; *T. cruzi*, amastigotes proliferating in 3T3 fibroblast cells; macrophage, mouse primary peritoneal macrophages; EC_{50} and CC_{50}, half-maximum growth-inhibition concentration; F, oral bioavailability in mouse after administering single compound dose (20 mg kg^{-1}) as a suspension; CL, plasma clearance in mouse after single i.v. bolus dose (5 mg kg^{-1}); ND, not determined; all EC_{50} and CC_{50} values correspond to means ± s.e.m. ($n = 4$ technical replicates).

Khare et al 2016

STOPP

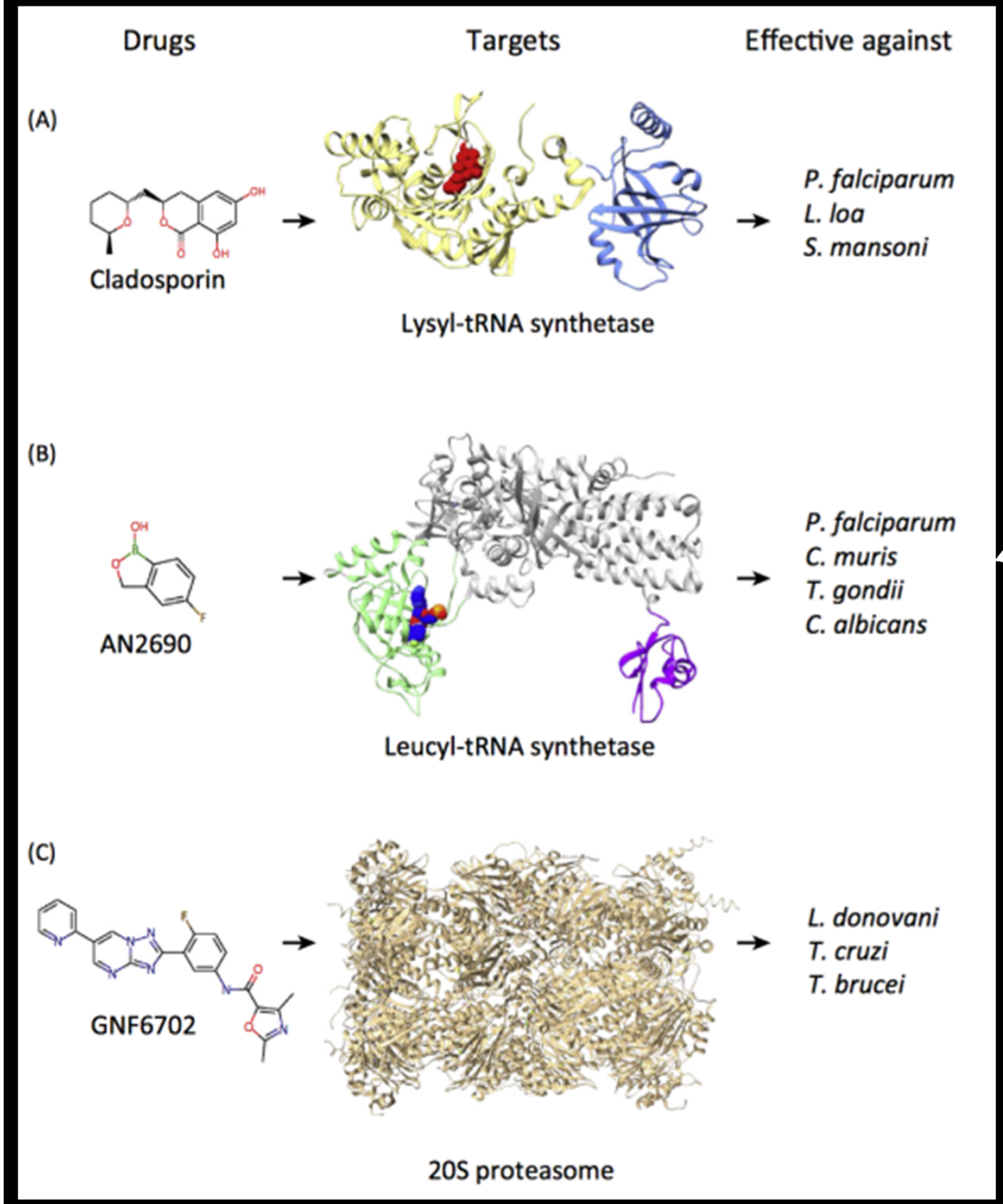

Translation

Degradation

Sharma et al, 2016, Jain et al, 2016, 2017

Plasmodium falciparum aaRSs

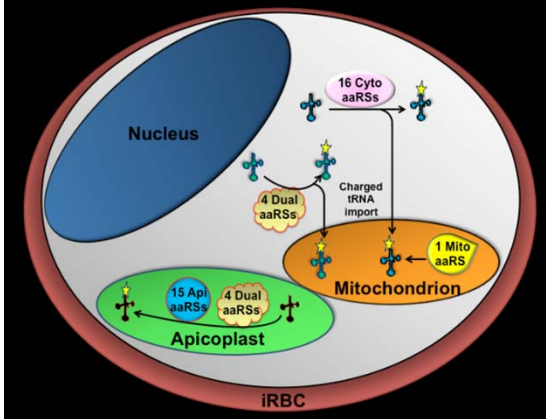

1 DRS	2 ERS	3 FRS	4 HRS	5 IRS	6 KRS	7 LRS	8 MRS
9 NRS	10 PRS	11 RRS	12 SRS	13 VRS	14 WRS	15 YRS	16 FRS 44%
		17 ARS 37%	18 CRS 38%	19 GRS 44%	20 TRS 53%		
21 DRS 48%	22 ERS 40%	23 FRS α-42% β-35%	24 HRS 48%	25 IRS 46%	26 KRS 55% 4H02	27 LRS 31% 5FOC	28 MRS 23%
29 NRS 33%	30 PRS 51% 4TWA	31 QRS 38%	32 RRS 30% 5JLD	33 SRS 41%	34 VRS 41%	35 WRS 44% 4JFA	36 YRS 34%

Apicoplast | Mitochondria | Cytoplasm | Dual: Ap + Cy

Pf-aaRSs: adaptable, high throughput assays:

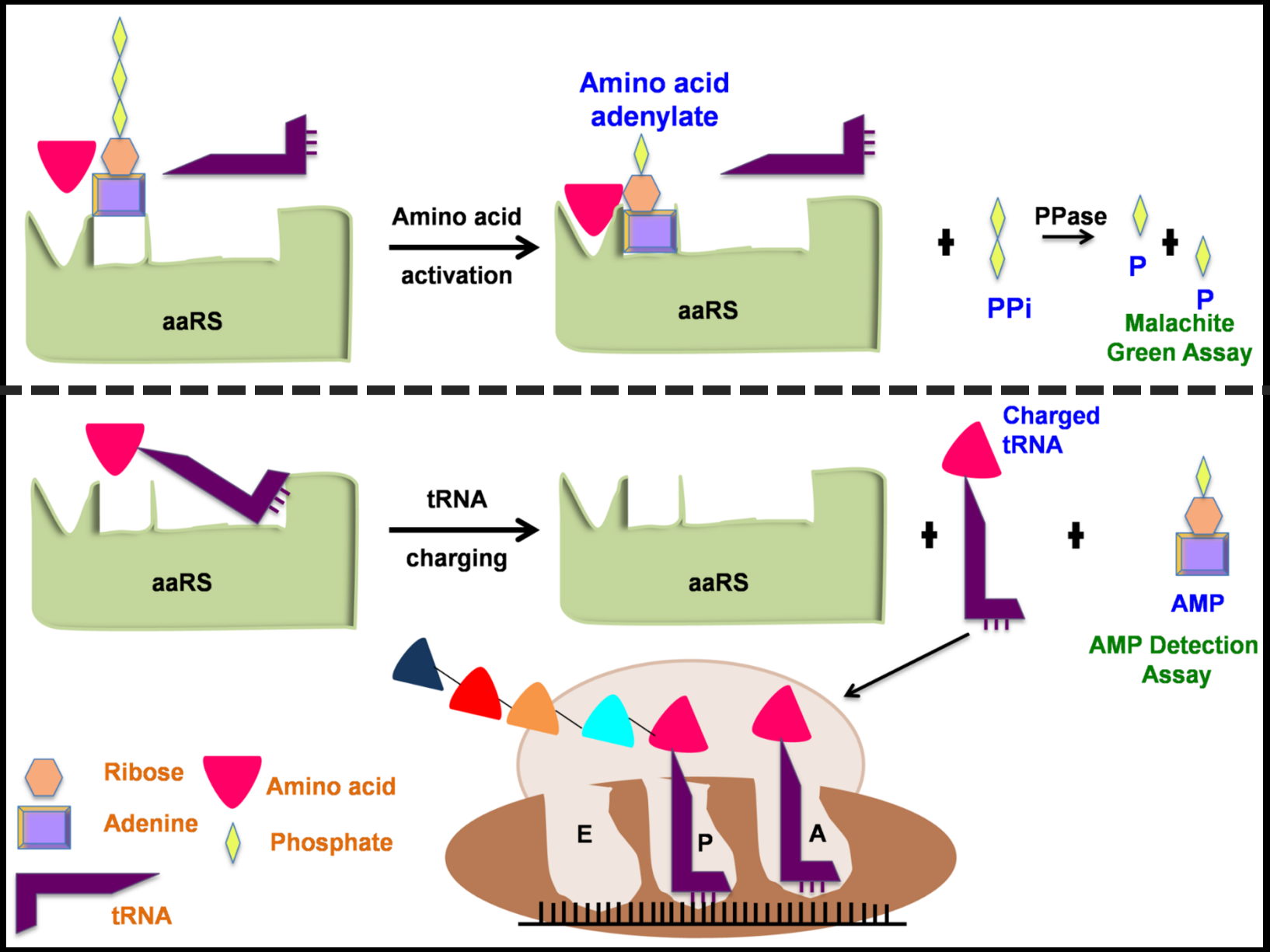

Pf-aaRSs: multiple targets and multi-targeting

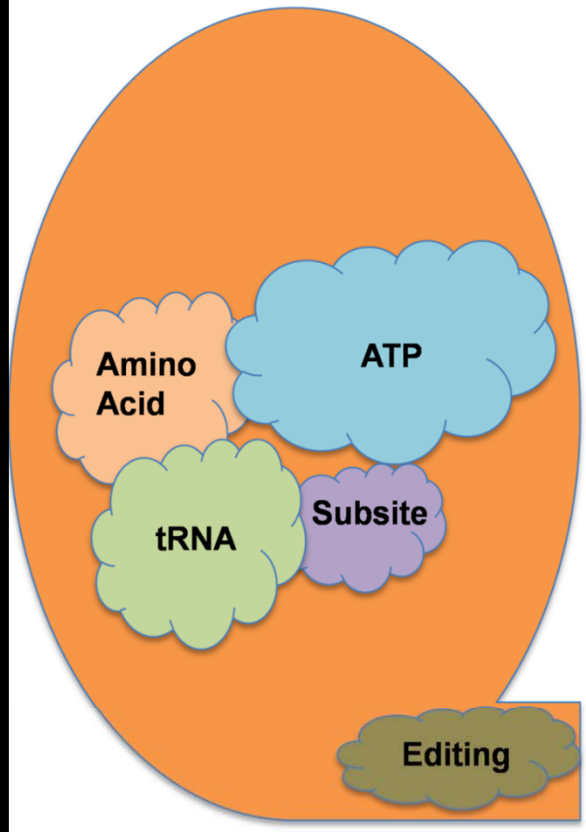

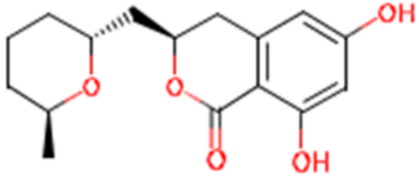

Cladosporin

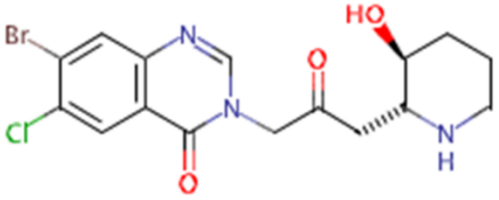

Halofuginone

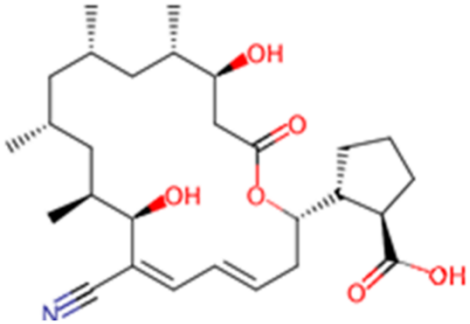

Borrelidin (BN)

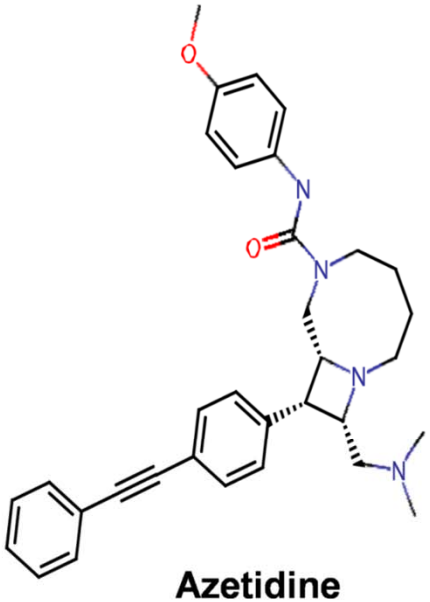

Azetidine (BRD7929)

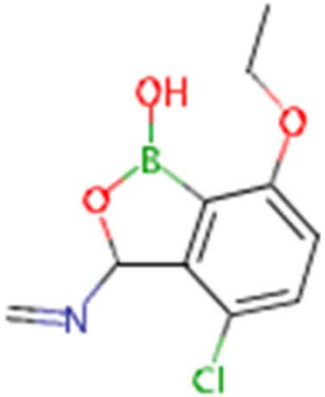

Benzoxaborole (AN6426)

Pf-aaRSs: subsites

Scaffold and aaRS	tRNA pocket	Amino acid pocket	ATP pocket	Subsite	Editing site pocket	IC50 (nM)	EC50 (nM)	References
Cladosporin KRS			+			61 in 3D7	48 in 3D7	Hoefpner et al, 2012
Halofuginone PRS	+	+				9 in 3D7	1 in 3D7	Jain et al, 2015
Benzoxaborole (AN6426) LRS					+	310 in W2	190 in 3D7	Sonoiki et al, 2006
Borrelidin TRS	+	+	+	+		0.9-7	1.8 in FCR3	Fang et al, 2015
Azetidine (BRD7929) FRS						23	9 in Dd2	Kato N et al, 2016

Pf-aaRSs: subsite occupancies

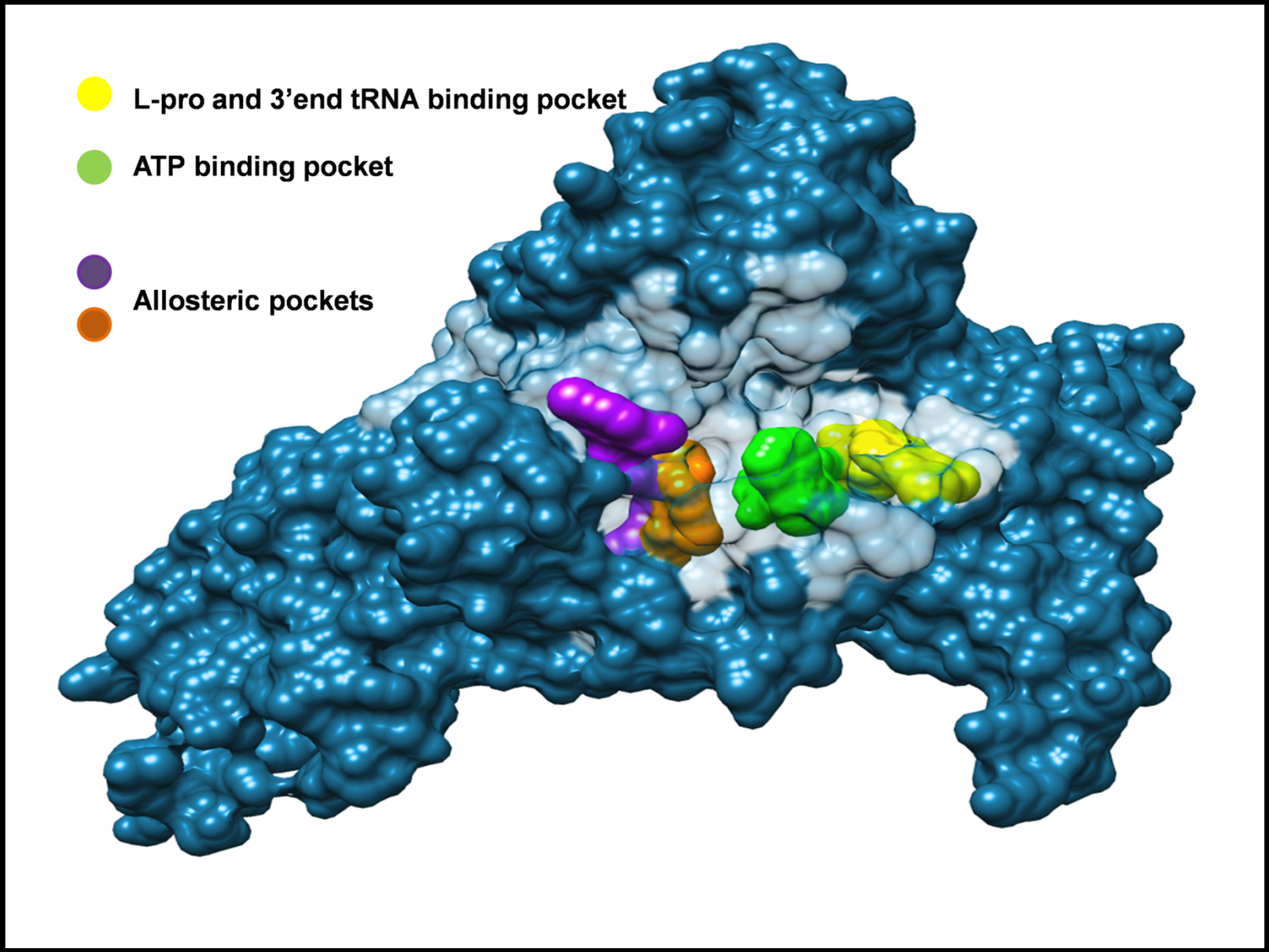

All thanks to:

Vitul Jain
Manickam Yogavel
Palak Babbar
Nipun Malhotra
Rini Chaturvedi
Manmohan Sharma

Dundee University, UK
CNRS, Grenoble, France
SGC (SDDC), Canada
Broad Institute, USA
Tohuku University, Japan
NCL, Pune

Wellcome Trust
European Union
GHIT, MMV
DST, DBT

Cladosporin in its avatars

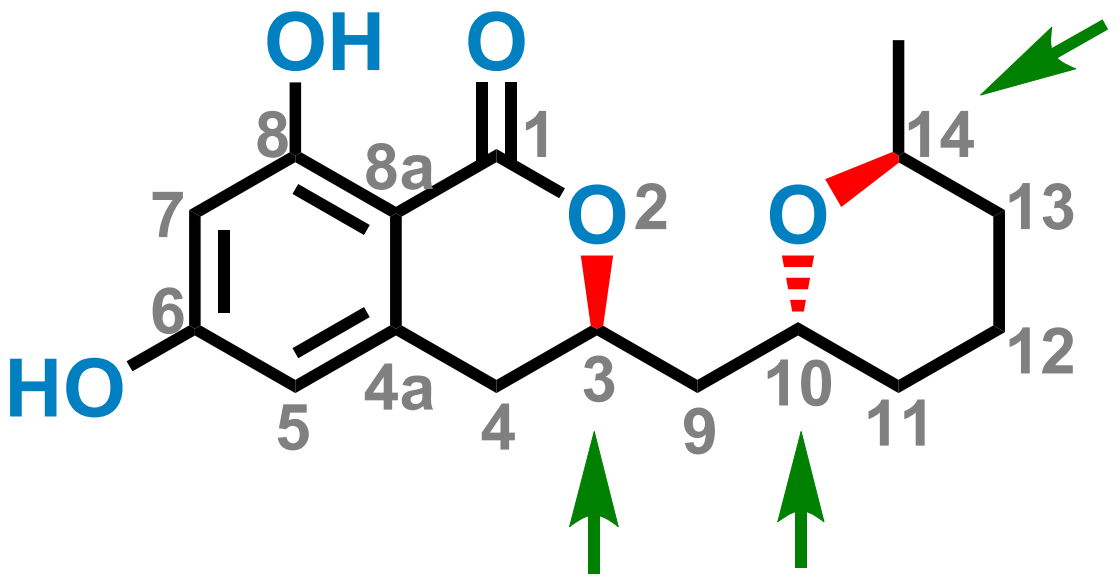

Structure of Cladosporin

Cladosporin in its avatars

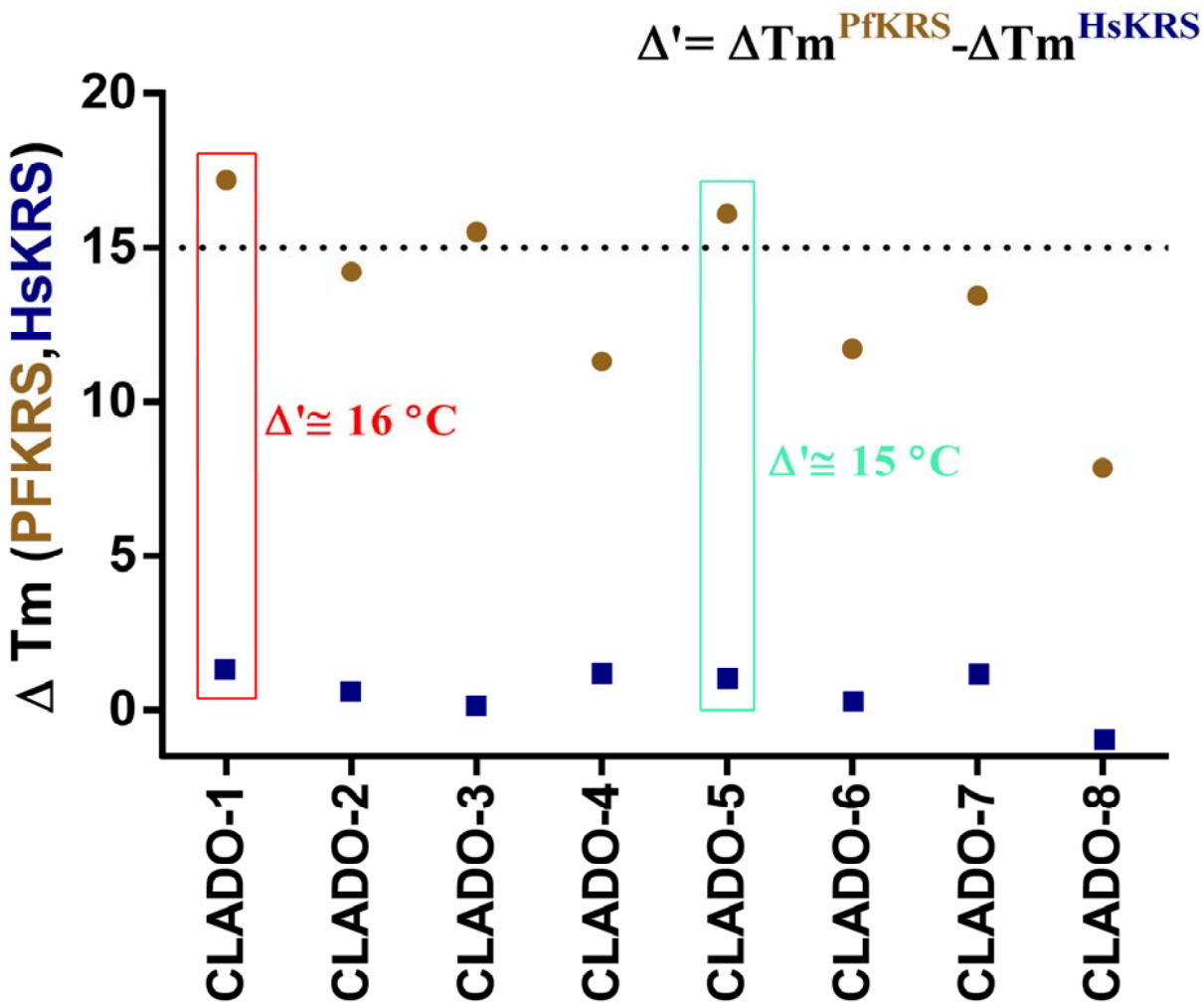

Cladosporin in its avatars

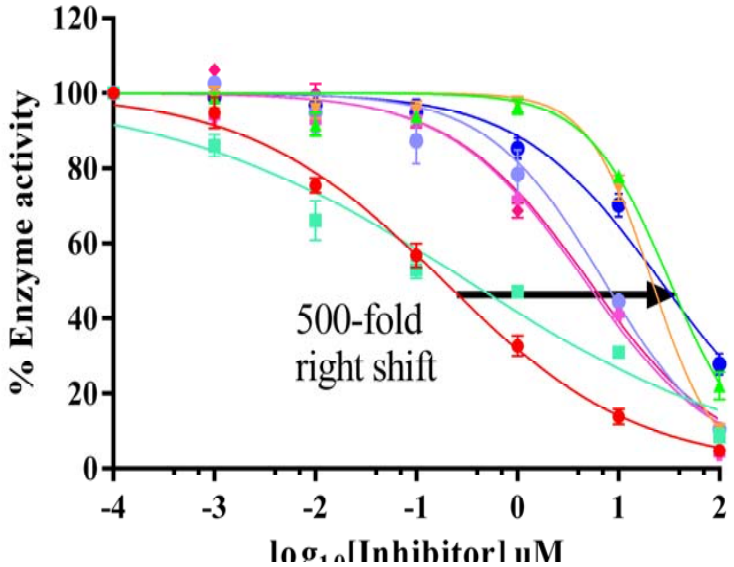

COMPOUND	IC_{50} PfKRS:HsKRS
CLADO-1:	0.12 ± 0.02:105± 2 uM
CLADO-2:	4.64 ± 0.5: >100 uM
CLADO-3:	5.8 ± 0.2: >100 uM
CLADO-4:	29 ± 4: >100 uM
CLADO-5:	0.29 ± 0.04: >100 uM
CLADO-6:	21.3 ± 2: >100 uM
CLADO-7:	7.25 ± 0.5: >100 uM
CLADO-8:	50± 5: >100 uM

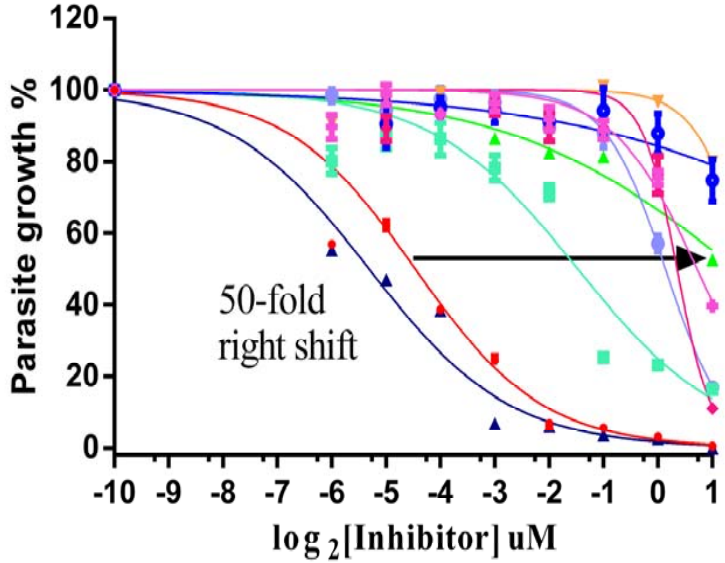

COMPOUND	EC_{50} PfKRS
CLADO-1:	≈ 0.04 uM
CLADO-2:	1.6 ± 0.1 uM
CLADO-3:	1.1 ± 0.1 uM
CLADO-4:	>2 uM
CLADO-5:	0.27 ± 0.02 uM
CLADO-6:	>2 uM
CLADO-7:	1.15 ± 0.05 uM
CLADO-8:	>2 uM
CHLOROQUINE:	≈ 0.02uM

Cladosporin in its avatars

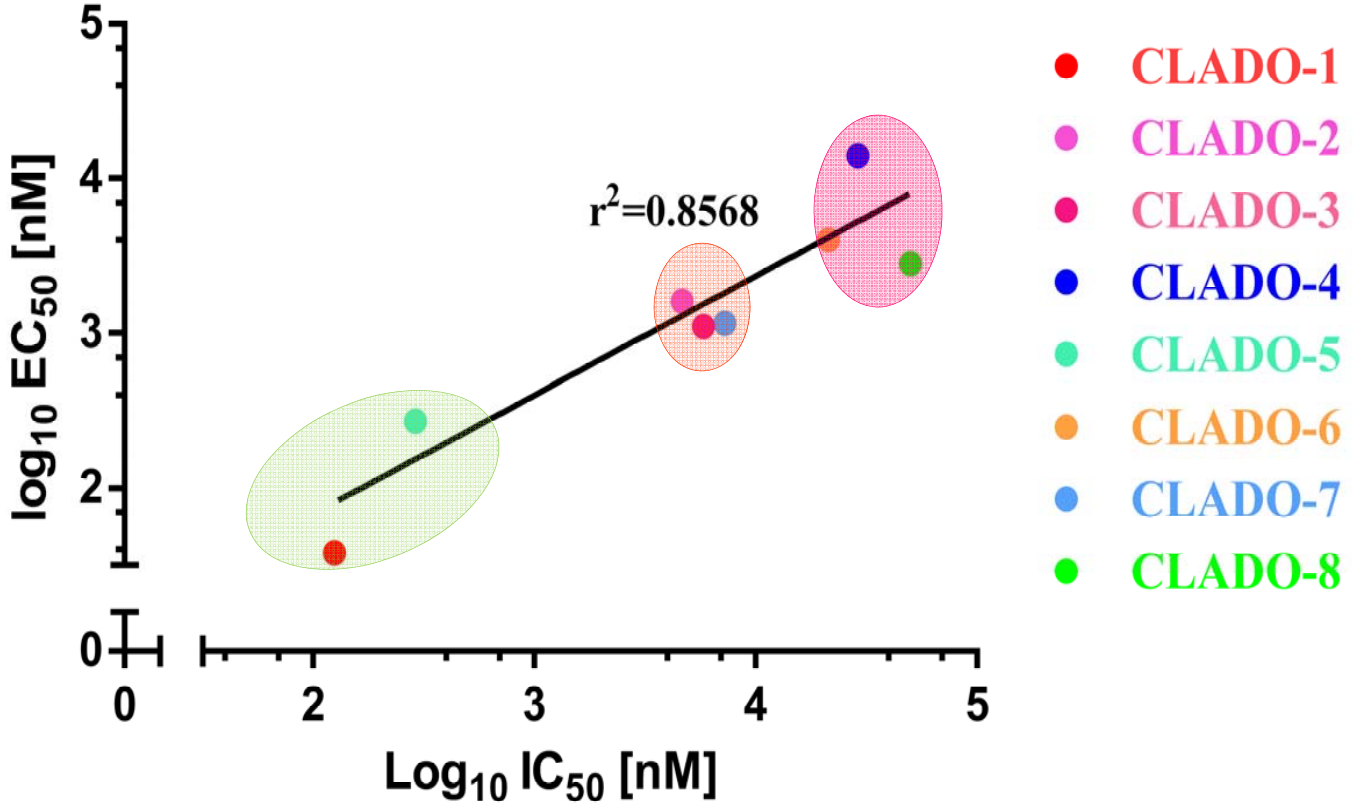

STOPP via GNF compounds: example 4

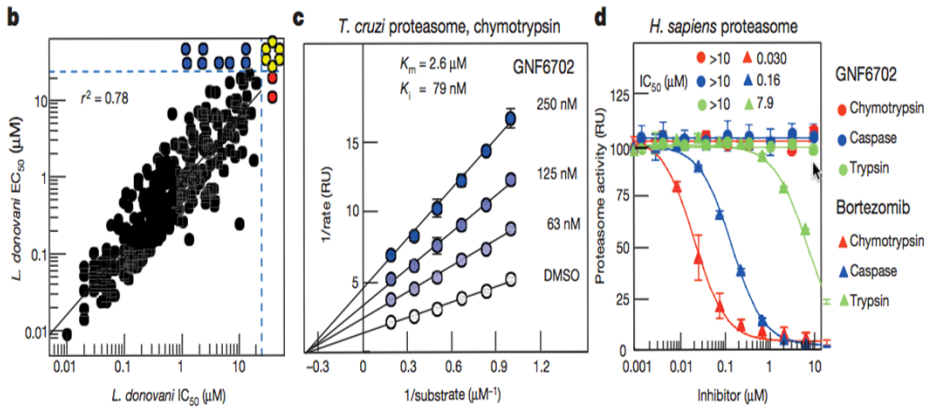

Figure 4 | Compounds from GNF6702 series inhibit growth of kinetoplastid parasites by inhibiting parasite proteasome chymotrypsin-like activity. a, Inhibition of three proteolytic activities of purified wild-type ($PSMB4^{WT}$) and $PSMB4^{I29M}$ *T. cruzi* proteasomes by GNF6702 and bortezomib; IC_{50} values for proteasome proteolytic activities are listed inside plots. **b,** Correlation between inhibition of chymotrypsin-like activity of purified *L. donovani* proteasome (IC_{50}) and *L. donovani* axenic amastigote growth inhibition (EC_{50}; data points correspond to means of 2 technical replicates); red circles, $IC_{50} > 20\,\mu M$; blue circles, $EC_{50} > 25\,\mu M$; yellow circles, $IC_{50} > 20\,\mu M$ and $EC_{50} > 25\,\mu M$; data for 317 analogues are shown. **c,** Lineweaver–Burk plot of inhibition of *T. cruzi* proteasome chymotrypsin-like activity by GNF6702 at increasing concentrations of a peptide substrate. **d,** Effect of GNF6702 and bortezomib on three proteolytic activities of human constitutive proteasome; IC_{50} values for proteasome proteolytic activities are listed inside plots. Data shown in **a**, **c** and **d** represent means ± s.e.m. ($n = 3$ technical replicates; for data points lacking error bars, s.e.m. values are smaller than circles representing means). Owing to limited aqueous solubility, the highest tested GNF6702 concentration in experiments shown in **a** and **d** was 10 μM.

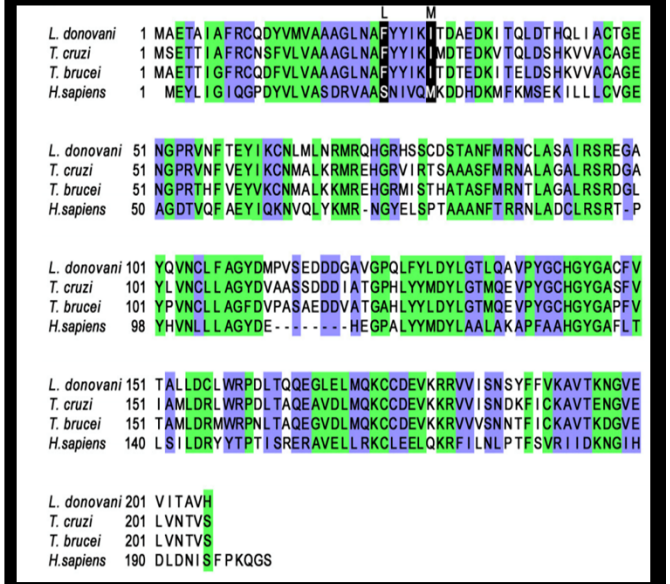

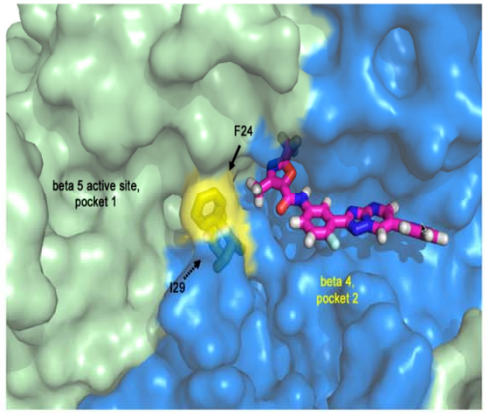

Extended Data Figure 6 | Hypothetical model of GNF6702 binding to *T. cruzi* proteasome β4 subunit. a, Alignment of amino acid sequences of proteasome β4 subunits (PSMB4) from *L. donovani*, *T. cruzi*, *T. brucei* and *Homo sapiens*. Green, amino acid residues conserved between human and kinetoplastid PSMB4 proteins; blue, amino acid residues conserved only among kinetoplastid PSMB4 proteins; black, amino acids mutated in *T. cruzi* mutants resistant to analogues from the GNF6702 series. **b,** Surface representation of the modelled *T. cruzi* 20S proteasome structure showing relative positions of the β5 and β4 subunits. β4 amino acid residues F24 and I29 (coloured yellow) are located at the interface of the two β subunits. GNF6702 is depicted in a sphere representation bound into a predicted pocket on the β4 subunit surface with carbon, nitrog oxygen and hydrogen atoms coloured magenta, blue, red and grey, respectively. The other *T. cruzi* 20S proteasome subunits are coloured grey. **c,** Close-up of the β5 and β4 subunits. The β5 subunit active site (pocket 1, chymotrypsin-like activity) is coloured pale green. The predicted β4 pocket (pocket 2) with bound GNF6702 is coloured blue The inhibitor is shown in a stick representation with atoms coloured described in caption for **b.** β4 residues F24 and I29 are coloured yello The proteasome model shown in **b** and **c** was produced in the PyMol Molecule Graphics System, Version 1.8, Schrodinger, LLC.